APPROXIMATE SEPARABILITY OF THE GREEN'S FUNCTIONS OF THE HELMHOLTZ EQUATION IN THE HIGH FREQUENCY LIMIT

BJÖRN ENGQUIST AND HONGKAI ZHAO

Abstract. The minimum number of terms needed in a separable approximation for a Green's function reveals the intrinsic complexity of the solution space of the underlying differential equation. It also has implications for whether low rank structures exist in the linear system after numerical discretization. The Green's functions for coercive elliptic differential operators in divergence form were shown to be highly separable [2] and efficient numerical algorithms exploiting low rank structures of the discretized systems were developed. In this work, a new approach to study the approximate separability of the Green's functions of the Helmholtz equation in the high frequency limit is developed. We show (1) lower bounds based on an explicit characterization of the correlation between two Green's functions and a tight dimension estimate for the best linear subspace to approximate a set of highly decorrelated Green's functions, (2) upper bounds based on constructing problem specific separable approximations, (3) sharpness of these bounds for a few case studies of practical interest.

1. Introduction

Given a linear differential operator, denoted by L, the Green's function, denoted by $G(\mathbf{x},\mathbf{y})$, is defined as the fundamental solution in an open domain $\Omega \subseteq R^d$ to the partial differential equation (PDE)

$$\begin{cases} L_x G(\mathbf{x},\mathbf{y}) = \delta(\mathbf{x}-\mathbf{y}), \quad \mathbf{x},\mathbf{y} \in \Omega \subseteq R^d \\ \\ \text{with boundary condition or condition at infinity,} \end{cases} \tag{1}$$

where $\delta(\mathbf{x}-\mathbf{y})$ is the Dirac delta function denoting a point source at $\mathbf{y}$. Any solution to the partial differential equation can be obtained by superpositions of the Green's functions with certain source distribution in Ω (and/or boundary $\partial\Omega$). $G(\mathbf{x},\mathbf{y})$ depends on two variables, the observation point $\mathbf{x}$ and the source point $\mathbf{y}$. The approximate separability of $G(\mathbf{x},\mathbf{y})$ is defined as the following: given two sets $X, Y \subseteq \Omega \subseteq R^d$ and $\epsilon > 0$, there is a

The work of Björn Engquist is partially supported by NSF grant DMS-1217203 and Texas Consortium for Computational Seismology.

The work of Hongkai Zhao is partially supported by NSF grant DMS-1115698 and ONR grant N00014-11-1-0602.

smallest N^ϵ such that there are $f_l(\mathbf{x}), g_l(\mathbf{y}), \mathbf{x} \in X, \mathbf{y} \in Y, l = 1, 2, \ldots, N^\epsilon$

$$\left\| G(\mathbf{x}, \mathbf{y}) - \sum_{l=1}^{N^\epsilon} f_l(\mathbf{x}) g_l(\mathbf{y}) \right\|_{X \times Y} \leq \epsilon, \quad \mathbf{x} \in X, \mathbf{y} \in Y, \tag{2}$$

where $\| \cdot \|_{X \times Y}$ is the norm of some function space to which G, f_l, g_l belong.

If one views $G(\mathbf{x}, \mathbf{y})$ as a family of functions in some function space defined on X with norm $\| \cdot \|_X$ and parameterized by $\mathbf{y} \in Y$ (the role of $\mathbf{x}$ and $\mathbf{y}$ can be reversed if reciprocity holds), this is related to the Kolmogorov n-width [1] [18] for this family of functions in the function space. Any linear subspace of the function space that approximates this family of functions to the tolerance ϵ has a dimension of at least N^ϵ and the space spanned by $f_l(\mathbf{x}), l = 1, 2, \ldots, N^\epsilon$ is an optimal one. Since any solution to the PDE can be represented as superpositions of the Green's functions, N^ϵ also manifests the intrinsic complexity of the solution space of the PDE within ϵ-approximation.

If X and Y are compact and disjoint domains in R^d and $G(\mathbf{x}, \mathbf{y})$ is continuous on $X \times Y$, one possible separable approximation is using polynomials by the Weierstrass Theorem. In other words, the polynomial basis are used to approximate the family of Green's functions. One can also use Fourier basis to construct separable approximations of the Green's functions. Problem specific separable approximations can be constructed as well. For example, if $G(\mathbf{x}, \mathbf{y})$ is $C^m(X \times Y)$ for two disjoint compact domains $X, Y \subset R^d$, it can be easily shown that a separable approximation of $G(\mathbf{x}, \mathbf{y})$ can be constructed using interpolations of a set of properly sampled Green's functions of the PDE, i.e., $f_l(x) = G(\mathbf{x}, \mathbf{y}_l), \mathbf{y}_l \in Y, l = 1, 2, \ldots, O(\epsilon^{-\frac{d}{m}})$. Similarly, the eigenfunctions of the differential operator can be used to construct separable approximations (see Remark 3.6). As we shall see these problem specific separable approximations can provide sharp upper bound estimates for the approximate separability. However, a sharp lower bound estimate for the approximate separability is much harder since intrinsic properties and structures independent of the choice of basis have to be used.

In the literature, the studies and results on the approximate separability of Green's functions were mainly aimed at upper bound estimates to show high separability, typical of the form $N^\epsilon \leq O(|\log \epsilon|^p)$ for some $p > 0$. Most of these upper bound estimates were obtained by constructing explicit separable approximations using polynomials and asymptotic expansions for special Green's functions with analytical formulas [12, 13, 28, 29, 26, 9, 7]. A more general mathematical approach was developed in [2]. It was shown that the Green's functions for coercive elliptic PDEs in divergence form with L_∞ coefficients are highly separable with $\mathbf{x}, \mathbf{y}$ belonging to two disjoint compact domains $X, Y \subset R^d$ respectively. It was proved, using a key gradient estimate by the Caccioppoli inequality, that $N_\epsilon \leq C|\log \epsilon|^{d+1}$ for some constant $C > 0$ that depends on the coefficients, the

[1] Kolmogorov n-width of a set S in a normed space W is its distance to the best n dimensional linear subspace L_n:

$$d_n(S, W) := \inf_{L_n} \sup_{f \in S} \inf_{g \in L_n} \|f - g\|_W,$$

separation distance between X and Y and the dimension d. Some interesting studies based on the free space Green's functions of the Helmholtz equation in the engineering literature [5, 6] showed that the scattered field is almost band limited and the degree of freedom is close to the Nyquist number in terms of the effective (spatial) bandwidth of the scattered field and to the extension of the observation domain.

In this work, we study the approximate separability of the Green's functions of the Helmholtz equation

$$\Delta_{\mathbf{x}} G(\mathbf{x},\mathbf{y}) + k^2 n^2(\mathbf{x}) G(\mathbf{x},\mathbf{y}) = \delta(\mathbf{x}-\mathbf{y}), \quad \mathbf{x},\mathbf{y} \in R^d, \tag{3}$$

as the wave number $k \to \infty$. Here $n(\mathbf{x})$, $0 < c < n(\mathbf{x}) < C < \infty$, is the index of refraction and $n(\mathbf{x}) - 1$ has a compact support. $G(\mathbf{x},\mathbf{y})$ satisfies the standard far field radiation condition. The method developed in [2] does not apply to the Helmholtz equation with large k, which becomes a singularly perturbed problem. The gradient of the Green's function of the Helmholtz equation becomes unbounded almost everywhere as $k \to \infty$ due to fast oscillations. In our study we derive asymptotic estimates for the minimum number of terms needed for a separable approximation of the Green's function N_k^ϵ (defined in (2)), as $k \to \infty$, where the added subindex emphasizes its dependence on k. We first clarify a few settings and define a few notations and then summarize our main results.

- The two sets X, Y are compact manifolds embedded in R^d with dimensions $\dim(X)$ and $\dim(Y)$ respectively. For examples, either one of them can be a compact domain, a compact two dimensional surface or a compact one dimensional curve in R^3. Without loss of generality, we assume $\dim(X) \geq \dim(Y) = s$.
- L_2 norm, denoted by $\|\cdot\|_2$, is used for the approximate separability defined in (2) in our analysis, which directly corresponds to the use of 2-norm for the singular value decomposition (SVD) of matrices in discrete cases.
- We present our results and proofs for the free space Green's function, denoted by $G_0(\mathbf{x},\mathbf{y})$, of the Helmholtz equation (3) in a homogeneous medium ($n(\mathbf{x}) \equiv 1$) in two and three dimensions. X and Y can overlap due to L_2 integrability of the Green's function at the source singularity. Our results extend to the Green's functions of the Helmholtz equation in heterogeneous media if a geometric optics Ansatz is valid. Our results also extend to the Green's functions of the Helmholtz equation in higher dimensions if X and Y are disjoint.
- The following relations are used to simplify notations: $x \gtrsim y$ means that there is a constant $\infty > c > 0$ such that $x \geq cy$, $x \lesssim y$ means that there is a constant $\infty > C > 0$ such that $x \leq Cy$, and $x \sim y$ means there are two constants $0 < c \leq C < \infty$ such that $cy \leq x \leq Cy$. For our asymptotic results, all constants are independent of the wave number k as $k \to \infty$. Dependence of these constants on other factors will be specified during the proofs.
- The Euclidean distance between two points $\mathbf{y}_1, \mathbf{y}_2 \in R^d$ is denoted by $|\mathbf{y}_1 - \mathbf{y}_2|$.

Our main results are:

- A characterization of the correlation (or angle) between two Green's functions of the Helmholtz equation (3) in the high frequency limit: there is some $\alpha > 0$,

$$(\|G_0(\cdot, \mathbf{y}_1)\|_2 \|G_0(\cdot, \mathbf{y}_2)\|_2)^{-1} \left| \int_X G_0(\mathbf{x}, \mathbf{y}_1) \overline{G}_0(\mathbf{x}, \mathbf{y}_2) d\mathbf{x} \right| \lesssim (k|\mathbf{y}_1 - \mathbf{y}_2|)^{-\alpha}$$

  as $k|\mathbf{y}_1 - \mathbf{y}_2| \to \infty$. Generically $\alpha = (\dim(X) \pm 1)/2$ depending on the relative locations of $\mathbf{y}_1, \mathbf{y}_2$ with respect to X (see Theorem 2.1).
- Lower and upper bound estimates for the approximate separability for the Green's functions of the Helmholtz equation in the high frequency limit: for two fixed compact manifolds X and Y with $\dim(X) \geq \dim(Y) = s$,

$$N_k^\epsilon \gtrsim \begin{cases} k^{2\alpha}, & \alpha < \frac{s}{2}, \\ \\ k^{s-\delta}, & \alpha \geq \frac{s}{2}, \end{cases}$$

  and

$$N_k^\epsilon \lesssim k^{s+\delta},$$

  as $k \to \infty$ for any $\delta > 0$ (see Lemma 3.1 and Theorem 3.1 - 3.4). Both estimates are sharp if $\alpha \geq \frac{s}{2}$, which occurs in many practical situations, e.g., X, Y are boundaries ($\dim(X) = \dim(Y) = s = 2$) of scatterers in three dimensions.
- Explicit estimates for the approximate separability of the Green's functions of the Helmholtz equation and their sharpness for situations that are commonly used in practice. These include cases with fixed X, Y, which are not highly separable, and highly separable cases with k dependent X, Y, e.g., the setting for the butterfly algorithm (see Section 4).

Approximate separability of Green's functions has direct and important implications for the development of efficient numerical algorithms. High separability implies the existence of low rank approximations for (sub)matrices of the corresponding discrete systems. Low rank structures can be exploited for matrix compression and design of efficient solvers. For examples, low rank approximations of dense (sub)matrices are used for fast matrix vector multiplication when solving boundary integral equations [9, 12, 13, 28, 29] and for the evaluation of scattering operators and Fourier integral operators [7, 26, 27]. Efficient numerical algorithms can also be developed for solving linear systems $Ax = b$ resulted from a discretization of a PDE by utilizing low rank approximations of off-diagonal submatrices such as hierarchical matrix method and structured inverse method [2, 4, 8, 16, 25, 31, 33, 34]. Since columns of A^{-1} are numerical approximations of the Green's functions of the corresponding PDE, the existence of low rank approximation of off-diagonal submatrices of A^{-1} is implied by high separability of the Green's functions $G(\mathbf{x}, \mathbf{y})$ with $x \in X, \mathbf{y} \in Y$ for some disjoint sets X and Y. Often in practice low rank approximations need to be computed. If a matrix is known to have a low rank approximation a priori, fast algorithms [15, 24] are available to compute a low rank approximation. However, the computation cost increases dramatically as the rank grows. So sharp estimates of both upper and lower bounds of the approximate separability of Green's functions is important in these applications.

It is well known that the Helmholtz equation with large wave number is notorious difficult to solve numerically. Our study here gives another mathematics perspective by showing that the lower bound for the approximate separability of the Green's functions of the Helmholtz equation grows as some power of the wavenumber k as $k \to \infty$. In other words, the intrinsic degrees of freedom needed to approximate the solution space of the Helmholtz equation to a given accuracy grows as some power of k.

As far as we know, our lower bound estimate for the approximate separability of Green's functions is the first in the literature. The lower bound estimate, which is sharp in many practical setups, characterizes the intrinsic complexity for high frequency wave phenomena mathematically. We hope these studies and understandings can provide useful insights for developing fast numerical algorithms as well.

2. Correlation between two Green's functions of the Helmholtz equation in the high frequency limit.

For completeness, we first provide the explicit formulas for the free space ($n(\mathbf{x}) \equiv 1$) Green's functions, denoted by $G_0(\mathbf{x}, \mathbf{y})$, of the Helmholtz equation (3) in any space dimension d.

$$G_0(\mathbf{x}, \mathbf{y}) = c_d k^p \frac{H_p^{(1)}(k|\mathbf{x}-\mathbf{y}|)}{|\mathbf{x}-\mathbf{y}|^p}, \quad p = \frac{d-2}{2}, \quad c_d = \frac{1}{2i(2\pi)^p}, \quad \mathbf{x}, \mathbf{y} \in R^d, \mathbf{x} \neq \mathbf{y}. \tag{4}$$

$H_p^{(1)}(r)$ is the first kind Hankel function of order p which has the following asymptotic behavior,

$$H_p^{(1)}(r) = \begin{cases} -\frac{i}{\pi}\Gamma(p)\left(\frac{2}{r}\right)^p, & p \neq 0 \\ \frac{2i}{\pi}\log r, & p = 0 \end{cases} \quad \text{as } r \to 0, \tag{5}$$

where $\Gamma(p)$ is the Gamma function, and

$$H_p^{(1)}(r) = \left(\frac{2}{\pi r}\right)^{\frac{1}{2}} e^{i(r - \frac{p\pi}{2} - \frac{\pi}{4})} + O(r^{-\frac{3}{2}}), \quad p \geq 0, \quad \text{as } r \to \infty. \tag{6}$$

For $d = 3$, the Green's function takes the simplest form

$$G_0(\mathbf{x}, \mathbf{y}) = \frac{1}{4\pi}\frac{e^{ik|\mathbf{x}-\mathbf{y}|}}{|\mathbf{x}-\mathbf{y}|}, \quad \mathbf{x} \neq \mathbf{y}. \tag{7}$$

For $d = 2$,

$$G_0(\mathbf{x}, \mathbf{y}) = -\frac{i}{4}H_0^{(1)}(k|\mathbf{x}-\mathbf{y}|) = -\frac{1}{2\pi}\int_0^\infty e^{ik|\mathbf{x}-\mathbf{y}|\cosh\theta} d\theta, \quad \mathbf{x} \neq \mathbf{y}, \tag{8}$$

and

$$\lim_{r\to 0^+} H_0^{(1)}(r) = \frac{2i}{\pi}\log r, \quad \lim_{r\to\infty} H_0^{(1)}(r) = \sqrt{\frac{2}{\pi r}} e^{i(r-\pi/4)} + O(r^{-3/2}). \tag{9}$$

Denote $B_\tau^d(\mathbf{y})$ and $S_\rho^d(\mathbf{y})$ to be a ball and a sphere in R^d centered at $\mathbf{y}$ with radius τ and ρ respectively. We have

$$\begin{aligned}\int_{B_\tau^n(\mathbf{y})} |G_0(\mathbf{x},\mathbf{y})|^2 d\mathbf{x} &= c_d^2 k^{2p} \int_0^\tau d\rho \int_{S_\rho^d} \frac{[H_p^{(1)}(k\rho)]^2}{\rho^{2p}} ds \\ &= c_d^2 \omega_d k^{2p-2} \int_0^{k\tau} r[H_p^{(1)}(r)]^2 dr,\end{aligned} \tag{10}$$

where $\omega_d = \frac{2\pi^{\frac{d}{2}}}{\Gamma(\frac{d}{2})}$ is the area of the unit sphere in R^d. From the asymptotic formula (5), it is easy to see that G_0 is square integrable at the singular source only for $d = 2, 3$ and $\|G_0(\cdot,\mathbf{y})\|_{2(B_\tau^n(\mathbf{y}))} \sim k^{\frac{d-3}{2}}$ as $k \to \infty$ from the asymptotic formula (6).

From the above explicit expressions for the free space Green's functions, it can be seen that except for the case $d = 3$, there is a scaling factor of some powers of k for the magnitude of the Green's function. To characterize the angle or correlation between two Green's functions with different source locations, we use the normalized Green's function for a given source point $\mathbf{y}$, denoted by $\hat{G}(\cdot,\mathbf{y})$,

$$\hat{G}(\cdot,\mathbf{y}) = \frac{G(\cdot,\mathbf{y})}{\|G(\cdot,\mathbf{y})\|_2}, \quad \mathbf{x} \in X \subset R^d, \quad \|G(\cdot,\mathbf{y})\|_2^2 = \int_X |G(\mathbf{x},\mathbf{y})|^2 d\mathbf{x}, \tag{11}$$

in our later study with the following understandings:

- $\|G(\cdot,\mathbf{y})\|_2$ is a smooth function of $\mathbf{y}$ since fast oscillations due to rapid change of the phase function is not present.
- When $d = 3$, all results for the normalized Green's function $\hat{G}(\mathbf{x},\mathbf{y})$ can be extended to $G(\mathbf{x},\mathbf{y})$ since there are constants $0 < c < C < \infty$ that are independent of k such that $c < \|G(\cdot,\mathbf{y})\|_2 < C, \forall \mathbf{y} \in Y$, where the constants depend on the sizes of the two compact domains $X, Y \subset R^3$ and the separation distance between them.

2.1. **Correlation between two Green's functions in the high frequency limit in a homogeneous medium.** When viewing $G(\mathbf{x},\mathbf{y})$ as a family of functions in $L_2(X)$ parameterized by $\mathbf{y} \in Y$, the separability condition (2) in $L_2(X \times Y)$ is equivalent to the existence of a linear subspace $S_X \subset L_2(X)$ with dimension N_k^ϵ such that

$$\sqrt{\int_Y \|G(\mathbf{x},\mathbf{y}) - P_{S_X} G(\mathbf{x},\mathbf{y})\|_{L_2(X)}^2 d\mathbf{y}} \le \epsilon, \tag{12}$$

where $P_{S_X} G(\mathbf{x},\mathbf{y})$ is the projection of $G(\mathbf{x},\mathbf{y})$ to S_X.

When 2-norm is used as the metric, one important geometric characterization of the relation between two vectors is the angle or correlation between them. Here we study the correlation between two Green's functions, $G(\mathbf{x},\mathbf{y}_1), G(\mathbf{x},\mathbf{y}_2)$, in term of the ratio of the separation distance between the two source points with respect to the wave length, i.e., $k|\mathbf{y}_1 - \mathbf{y}_2|$.

Since the correlation between two Green's functions of the Helmholtz equation in the high frequency limit involves highly oscillatory integrals, the following stationary phase lemma

[17, 32], which gives an explicit estimate of the error of the stationary phase approximation in terms of the fast oscillations and regularity of the integrand, will be used.

Lemma 2.1. *Let $I(k) = \int e^{ik\phi(\mathbf{x})}u(\mathbf{x})dx$, where $u \in \mathcal{C}_c^\infty(R^d)$ complex valued, with support in a compact set $K \subset R^d$, $\phi \in C^\infty(R^d)$ real valued and $k \geq 1$. If $\mathbf{x}_0$ is the only stationary point of ϕ in K and not degenerate, i.e., $|\nabla\phi(\mathbf{x}_0)| = 0$ and $D^2\phi(\mathbf{x}_0)$ is invertible, then*

$$
\begin{aligned}
&|I(k) - (\tfrac{2\pi}{k})^{d/2}\tfrac{e^{ik\phi(\mathbf{x}_0)}}{|\det[D^2\phi(\mathbf{x}_0)]|^{1/2}}e^{\frac{i\pi}{4}sgn(D^2\phi(\mathbf{x}_0))}\textstyle\sum_{j<p}k^{-j}L_ju(\mathbf{x}_0)| \\
&\leq Ck^{-d/2-p}|\det[D^2\phi(\mathbf{x}_0)]|^{-1/2}\|[D^2\phi(\mathbf{x}_0)]^{-1}\|^p\textstyle\sum_{|\beta|\leq 2p+q}\|D^\beta u\|_{L^2},
\end{aligned}
\tag{13}
$$

where L_j are differential operators of order $\leq 2j$, $q > d/2$ is an integer and C is an universal constant independent of ϕ and u.

In the following study we only need the above result for $p = 1$. However, the standard stationary phase results can not be applied directly due to the following complications in our case: (1) the stationary points may not be isolated, (2) the integration is on a compact domain X and the integrand u is not $C_0^\infty(X)$, and (3) there may be singularities in the integrand.

Theorem 2.1. *Given a fixed compact domain $X \subset R^d, d = 2, 3$ with piecewise smooth boundary, there is a α, $\frac{d-1}{2} \leq \alpha \leq \frac{d+1}{2}$, such that*

$$
\left| < \hat{G}_0(\cdot, \mathbf{y}_1), \hat{G}_0(\cdot, \mathbf{y}_2) >_X \right| \lesssim (k|\mathbf{y}_1 - \mathbf{y}_2|)^{-\alpha}, \quad \text{as } k|\mathbf{y}_1 - \mathbf{y}_2| \to \infty,
\tag{14}
$$

where $\hat{G}_0(\mathbf{x}, \mathbf{y})$ is the normalized free space Green's function of the Helmholtz equation. The constant in $\lesssim$ depends on X and the distances from $\mathbf{y}_1, \mathbf{y}_2$ to X.

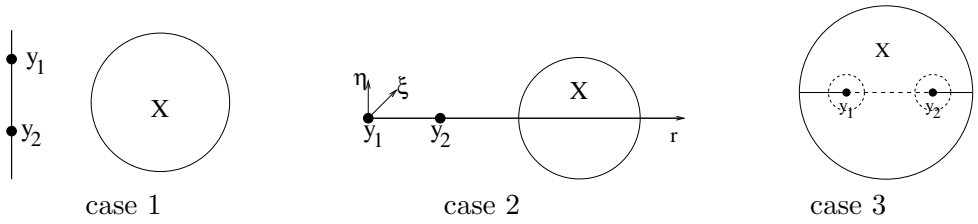

FIGURE 1. Different positions of $\mathbf{y}_1, \mathbf{y}_2$ relative to X

Proof. We prove for $d = 3$ first. Define

$$
\begin{aligned}
&\tilde{k} = k|\mathbf{y}_1 - \mathbf{y}_2|, \quad \tilde{\phi}(\mathbf{x}) = |\mathbf{y}_1 - \mathbf{y}_2|^{-1}(|\mathbf{x} - \mathbf{y}_1| - |\mathbf{x} - \mathbf{y}_2|), \\
&u(\mathbf{x}) = \tfrac{1}{\|G_0(\cdot,\mathbf{y}_1)\|_2\|G_0(\cdot,\mathbf{y}_2)\|_2|\mathbf{x}-\mathbf{y}_1||\mathbf{x}-\mathbf{y}_2|},
\end{aligned}
\tag{15}
$$

and the operator

$$L = \frac{1}{|\nabla\tilde{\phi}(\mathbf{x})|^2}\sum_{j=1}^{3}\frac{\partial\tilde{\phi}}{\partial x_j}\frac{\partial}{\partial x_j} \quad L^T = -\sum_{j=1}^{3}\frac{\partial}{\partial x_j}\frac{1}{|\nabla\tilde{\phi}(\mathbf{x})|^2}\frac{\partial\tilde{\phi}}{\partial x_j}. \tag{16}$$

Then

$$\left|< \hat{G}_0(\cdot,\mathbf{y}_1), \hat{G}_0(\cdot,\mathbf{y}_2) >\right| = \left|\int_X e^{i\tilde{k}\tilde{\phi}(\mathbf{x})}u(\mathbf{x})d\mathbf{x}\right| \tag{17}$$

We have $|\tilde{\phi}(\mathbf{x})| \le 1$ and

$$\begin{aligned}\nabla\tilde{\phi}(\mathbf{x}) &= |\mathbf{y}_1-\mathbf{y}_2|^{-1}\left(\tfrac{\mathbf{x}-\mathbf{y}_1}{|\mathbf{x}-\mathbf{y}_1|}-\tfrac{\mathbf{x}-\mathbf{y}_2}{|\mathbf{x}-\mathbf{y}_2|}\right)\\ D^2\tilde{\phi}(\mathbf{x}) &= |\mathbf{y}_1-\mathbf{y}_2|^{-1}\left[\frac{I-\frac{(\mathbf{x}-\mathbf{y}_1)}{|\mathbf{x}-\mathbf{y}_1|}\otimes\frac{(\mathbf{x}-\mathbf{y}_1)}{|\mathbf{x}-\mathbf{y}_1|}}{|\mathbf{x}-\mathbf{y}_1|}-\frac{I-\frac{(\mathbf{x}-\mathbf{y}_2)}{|\mathbf{x}-\mathbf{y}_2|}\otimes\frac{(\mathbf{x}-\mathbf{y}_2)}{|\mathbf{x}-\mathbf{y}_2|}}{|\mathbf{x}-\mathbf{y}_2|}\right],\end{aligned} \tag{18}$$

where $\otimes$ denotes the tensor product of two vectors.

Denote the line going through $\mathbf{y}_1,\mathbf{y}_2$ by $l_{\mathbf{y}_1}^{\mathbf{y}_2}$ and the part of $l_{\mathbf{y}_1}^{\mathbf{y}_2}$ outside the segment between $\mathbf{y}_1,\mathbf{y}_2$ by $\tilde{l}_{\mathbf{y}_1}^{\mathbf{y}_2}$. The gradient of $\tilde{\phi}$ only vanishes on $\tilde{l}_{\mathbf{y}_1}^{\mathbf{y}_2}$, where the maximum value 1 or the minimum value -1 of $\tilde{\phi}$ is attained. The Hessian $D^2\tilde{\phi}(\mathbf{x})$ is degenerate for $\mathbf{x}\in l_{\mathbf{y}_1}^{\mathbf{y}_2}$ in the direction of $\mathbf{y}_1-\mathbf{y}_2$. At any $\mathbf{x}\in l_{\mathbf{y}_1}^{\mathbf{y}_2}$, the Hessian restricted to the plane perpendicular to the line $l_{\mathbf{y}_1}^{\mathbf{y}_2}$, denoted by $D^2_\perp\phi(\mathbf{x})$, is a multiple of the identity matrix in the plane, denoted by $I_\perp$. In particular, for $\mathbf{x}\in\tilde{l}_{\mathbf{y}_1}^{\mathbf{y}_2}$,

$$D^2_\perp\tilde{\phi}(\mathbf{x}) = \frac{\pm 1}{|\mathbf{x}-\mathbf{y}_1||\mathbf{x}-\mathbf{y}_2|}I_\perp, \tag{19}$$

where the sign depends on whether the maximum or the minimum of $\tilde{\phi}$ is attained at $\mathbf{x}$.

Depending on the positions of $\mathbf{y}_1,\mathbf{y}_2$ relative to the domain X, we consider three generic cases illustrated in Figure 1. All other cases can be deduced from these three cases.

Case 1. $\tilde{l}_{\mathbf{y}_1}^{\mathbf{y}_2}\cap X=\emptyset$, see Figure 1. Since there is no stationary point in X, i.e., $|\nabla\tilde{\phi}(\mathbf{x})|>c>0,\forall\mathbf{x}\in X$, and $u(\mathbf{x})$ is smooth in X, from integration by part we have

$$\begin{aligned}&\textstyle\int_X e^{i\tilde{k}\tilde{\phi}(\mathbf{x})}u(\mathbf{x})d\mathbf{x} = \frac{1}{i\tilde{k}}\int_X(Le^{i\tilde{k}\tilde{\phi}(\mathbf{x})})u(\mathbf{x})d\mathbf{x}\\ &=\tfrac{1}{i\tilde{k}}\Big[\textstyle\int_X e^{i\tilde{k}\tilde{\phi}(\mathbf{x})}(L^Tu(\mathbf{x}))d\mathbf{x}+\int_{\partial X}|\nabla\tilde{\phi}(\mathbf{x})|^{-2}(\sum_{j=1}^3\nu_j\tfrac{\partial\tilde{\phi}}{\partial x_j})e^{i\tilde{k}\tilde{\phi}(\mathbf{x})}u(\mathbf{x})dS(\mathbf{x})\Big]\\ &=-\tfrac{1}{\tilde{k}^2}\Big[\textstyle\int_X e^{i\tilde{k}\tilde{\phi}(\mathbf{x})}((L^T)^2u(\mathbf{x}))d\mathbf{x}+\int_{\partial X}|\nabla\tilde{\phi}(\mathbf{x})|^{-2}(\sum_{j=1}^3\nu_j\tfrac{\partial\tilde{\phi}}{\partial x_j})e^{i\tilde{k}\tilde{\phi}(\mathbf{x})}L^Tu(\mathbf{x})dS(\mathbf{x})\Big]\\ &+\tfrac{1}{i\tilde{k}}\textstyle\int_{\partial X}|\nabla\tilde{\phi}(\mathbf{x})|^{-2}(\sum_{j=1}^3\nu_j\tfrac{\partial\tilde{\phi}}{\partial x_j})e^{i\tilde{k}\tilde{\phi}(\mathbf{x})}u(\mathbf{x})dS(\mathbf{x}).\end{aligned} \tag{20}$$

Integration by part can be continued. However, we show that the last term, which is an oscillatory integral on the boundary ∂X, is of the leading order. For a generic domain X,

the phase function $\tilde{\phi}(\mathbf{x})$ has isolated non-degenerate critical points on ∂X. The boundary integral in the last term is $\lesssim \tilde{k}^{-\frac{d-1}{2}}$ by the standard stationary phase theory. Hence

$$\left|\int_X e^{i\tilde{k}\tilde{\phi}(\mathbf{x})}u(\mathbf{x})d\mathbf{x}\right| \lesssim \tilde{k}^{-\frac{d+1}{2}} = \tilde{k}^{-2}, \quad \text{as } \tilde{k}\to\infty, \tag{21}$$

when $d=3$. The constant in $\lesssim$ comes from the use of stationary phase lemma 2.1 for the boundary integral. It depends on the values of $|\nabla\tilde{\phi}(\mathbf{x})|^{-2}(\sum_{j=1}^3 \nu_j \frac{\partial\tilde{\phi}}{\partial x_j})u(\mathbf{x})$ at the critical points of $\tilde{\phi}$ on ∂X, where $\tilde{\phi}$ and u are defined in (15). Since both $\tilde{\phi}$ and u depend on the relative positions of $\mathbf{y}_1, \mathbf{y}_2$ to X and on X, e.g., the size and the boundary, so is the constant.

In the special situation that a piece of the boundary ∂X coincides with a level set of $\tilde{\phi}(\mathbf{x})$, see Figure 2, the phase function $\tilde{\phi}(\mathbf{x})$ is constant on that piece, the boundary integral in the last term is $\lesssim 1$ and hence

$$\left|\int_X e^{i\tilde{k}\tilde{\phi}(\mathbf{x})}u(\mathbf{x})d\mathbf{x}\right| \lesssim \tilde{k}^{-1}, \quad \text{as } \tilde{k}\to\infty. \tag{22}$$

The constant in $\lesssim$ depends on the boundary integral, especially on the piece of ∂X that coincides with a level set of $\tilde{\phi}(\mathbf{x})$. Again the constant depends on the relative positions of $\mathbf{y}_1, \mathbf{y}_2$ to X and on X.

There are other special situations for case 1, e.g., the boundary ∂X touches a level set of $\tilde{\phi}(\mathbf{x})$ along a curve, the last term in (20) will be of order higher than $\tilde{k}^{-1}$.

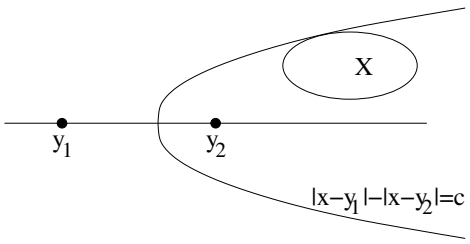

FIGURE 2. A piece of the boundary ∂X stays on a level set of $\tilde{\phi}(\mathbf{x})$

Case 2. $\mathbf{y}_1, \mathbf{y}_2$ are outside X but $\tilde{l}^{\mathbf{y}_2}_{\mathbf{y}_1} \cap X \neq \emptyset$, see Figure 1. Both $\tilde{\phi}(\mathbf{x})$ and $u(\mathbf{x})$ are smooth in X. In this situation, all points on the line segment $\tilde{l}^{\mathbf{y}_2}_{\mathbf{y}_1} \cap X$ are non-degenerate critical points with the same phase, $\tilde{\phi}(\mathbf{x}) \equiv \pm 1, \mathbf{x} \in \tilde{l}^{\mathbf{y}_2}_{\mathbf{y}_1}$. Introduce a new coordinate system (r, ξ, η), where the origin is at $\mathbf{y}_1$ and r-axis is in the direction $\mathbf{y}_1 - \mathbf{y}_2$, and (ξ, η) is an orthogonal system perpendicular to r. We have

$$\int_X e^{i\tilde{k}\tilde{\phi}(\mathbf{x})}u(\mathbf{x})d\mathbf{x} = \int_{r_1}^{r_2}\int_{X(r)} e^{i\tilde{k}\tilde{\phi}(r,\xi,\eta)}u(r,\xi,\eta)d\xi d\eta dr \tag{23}$$

where $X(r)$ denotes the intersection of X with the plane (r, ξ, η) at a fixed r and define $r_1 = \min_{(r,\xi,\eta)\in X} r,\ r_2 = \max_{(r,\xi,\eta)\in X} r$.

For a fixed $r \in [r_1, r_2]$, if $\tilde{l}^{\mathbf{y}_2}_{\mathbf{y}_1} \cap X(r) = (r, 0, 0)$, it is the only stationary point of $\tilde{\phi}$ in the plane (r, ξ, η) and

$$\begin{aligned} &\tilde{\phi}(r,0,0) = 1, \\ &D^2_{\xi\eta}\tilde{\phi}(r,0,0) = \tfrac{1}{r(|\mathbf{y}_1-\mathbf{y}_2|+r)} I, \\ &u_1(r,0,0)|_{\psi=0} = \tfrac{1}{\|G_0(\cdot,\mathbf{y}_1)\|_2 \|G_0(\cdot,\mathbf{y}_2)\|_2 r(|\mathbf{y}_1-\mathbf{y}_2|+r)}, \end{aligned} \tag{24}$$

where I is the 2×2 identity matrix. If $(r,0,0)$ is in the interior of $X(r)$, let $B_\tau(0) \subset X(r)$ be a small disc centered at $(r,0,0)$ with radius $\tau > 0$. Construct a partition of unity for the domain $X(r)$ in (ξ,η) plane: $\chi_1(r,\xi,\eta) + \chi_2(r,\xi,\eta) \equiv 1, \forall (r,\xi,\eta) \in X(r)$ such that $0 \le \chi_1(r,\xi,\eta) \le 1$ is smooth and is 1 in $B_\tau(0)$ and zero near the boundary of $\partial X(r)$. Denote $u_i = \chi_i u, i = 1, 2$, then

$$\int_{X(r)} e^{i\tilde{k}\tilde{\phi}(r,\xi,\eta)} u(r,\xi,\eta) d\xi d\eta = \int_{X(r)} e^{i\tilde{k}\tilde{\phi}(r,\xi,\eta)} u_1(r,\xi,\eta) d\xi d\eta + \int_{X(r)} e^{i\tilde{k}\tilde{\phi}(r,\xi,\eta)} u_2(r,\xi,\eta) d\xi d\eta \tag{25}$$

Since there is no stationary point in the second integral, one can use integration by part argument as in case 1 on the planar domain $X(r)$ to show that it is $\lesssim \tilde{k}^{-\frac{d}{2}}$ generically or at most $\lesssim \tilde{k}^{-1}$ in special cases. For the first integral, $(r,0,0)$ is the only stationary point. Apply the standard stationary phase result and from (24) we get

$$\left| \int_{X(r)} e^{i\tilde{k}\tilde{\phi}(r,\xi,\eta)} u_1(r,\xi,\eta) d\xi d\eta - \frac{2\pi i \tilde{k}^{-\frac{d-1}{2}} e^{i\tilde{k}}}{\|G_0(\cdot,\mathbf{y}_1)\|_2 \|G_0(\cdot,\mathbf{y}_2)\|_2} \right| \lesssim \tilde{k}^{-\frac{d+1}{2}} \tag{26}$$

It is important to note that the phase in the leading term after integration in (ξ,η) over $X(r)$ is independent of r, which means no fast oscillations when integrating in r. Combining the estimates for both terms on the righthand side of (25), we have

$$\left| \int_{X(r)} e^{i\tilde{k}\tilde{\phi}(r,\xi,\eta)} u(r,\xi,\eta) d\xi d\eta \right| \lesssim \tilde{k}^{\max\{-\frac{d}{2}, -\frac{d-1}{2}\}} = \tilde{k}^{-\frac{d-1}{2}}, \tag{27}$$

generically or at most $\tilde{k}^{-1}$.

In the special case that $(r,0,0) \in \partial X(r)$, i.e., $\tilde{l}^{\mathbf{y}_2}_{\mathbf{y}_1}$ touches $X(r)$ at $(r,0,0)$, again construct a partition of unity for $X(r)$ in (ξ,η) plane: $\chi_1(r,\xi,\eta) + \chi_2(r,\xi,\eta) \equiv 1, \forall (r,\xi,\eta) \in X(r)$. Let $B_\tau(0)$ be a small disc centered at $(r,0,0)$ with radius $\tau > 0$. $0 \le \chi_1(r,\xi,\eta) \le 1$ is smooth and $\chi_1(r,\xi,\eta) \equiv 1, \forall (r,\xi,\eta) \in B_\tau(0) \cap X(r)$. χ_1 goes to zero smoothly outside a region that is a little larger than $B_\tau(0) \cap X(r)$. One can use a similar argument as above to break the integration in X into two parts except that integration in the region containing the stationary point $(r,0,0)$ is different. Instead of integration in a disc around the stationary point, where the stationary lemma can be directly applied, the integration region around the stationary point is $B_\tau(0) \cap X(r)$. As $\tilde{k} \to \infty$ the contribution of the stationary phase becomes more and more localized around the stationary point $(r,0,0)$. Since $\partial X(r)$ is smooth and, moreover, both the phase function $\tilde{\phi}$ and u are radial symmetric with respect to $(r,0,0)$ in (ξ,η) plane, the leading term of the integral is half of that of the

integral in a disc around the stationary point. In any case, estimate (27) is still valid for this special case.

For a fixed $r \in [r_1, r_2]$, if $\tilde{l}_{\mathbf{y}_1}^{\mathbf{y}_2} \cap X(r) = \emptyset$, there is no stationary point in $X(r)$. Hence it is reduced to a similar situation to Case 1, for which integration by part argument can be used to show that $\int_{X(r)} e^{i\tilde{k}\tilde{\phi}(r,\xi,\eta)} u_2(r,\xi,\eta) d\xi d\eta \lesssim \tilde{k}^{-\frac{d}{2}}$ generically or at most $\lesssim \tilde{k}^{-1}$ (in special cases). Combing the above scenarios, we have

$$\left| \int_X e^{i\tilde{k}\tilde{\phi}(\mathbf{x})} u(\mathbf{x}) d\mathbf{x} \right| = \left| \int_{r_1}^{r_2} \int_{X(r)} e^{i\tilde{k}\tilde{\phi}(r,\xi,\eta)} u(r,\xi,\eta) d\xi d\eta dr \right| \lesssim \tilde{k}^{-1}. \tag{28}$$

In a generic situation, if $\tilde{l}_{\mathbf{y}_1}^{\mathbf{y}_2}$ has line segment in X, the above estimate is $\lesssim \tilde{k}^{-\frac{d-1}{2}}$. In other words, the decorrelation rate is less than Case 1 due to the line of stationary phase $\tilde{l}_{\mathbf{y}_1}^{\mathbf{y}_2} \cap X$.

The constant in $\lesssim$ depends on: 1) the estimate for the first term on the righthand side of (25), which only depends on $\|G_0(\cdot, \mathbf{y}_1)\|_2 \|G_0(\cdot, \mathbf{y}_2)\|_2$ due to the use of stationary phase lemma in (26), and the estimate for the second term on the righthand side of (25), which is similar to case 1, for each fixed $r \in [r_1, r_2]$, and 2) the integration in r in the interval $[r_1, r_2]$. Hence, the constant still depends on the relative positions of $\mathbf{y}_1, \mathbf{y}_2$ to X and on X.

Case 3. $\mathbf{y}_1$ and (or) $\mathbf{y}_2$ are in the interior of X, see Figure 1. We show that the main contribution still comes from the line of stationary points $\tilde{l}_{\mathbf{y}_1}^{\mathbf{y}_2} \cap X$. However, singularities of u at $\mathbf{y}_1$ and $\mathbf{y}_2$ have to be taken care of. Take r_0, $0 < r_0 < |\mathbf{y}_1 - \mathbf{y}_2|/4$, small enough such that a ball with radius r_0 centered at $\mathbf{y}_1$ or $\mathbf{y}_2$ is contained in X. Let $\chi_0(\mathbf{x}), \chi_1(\mathbf{x}), \chi_2(\mathbf{x})$ be a partition of unity functions, each of which is smooth and non-negative and $\chi_0(\mathbf{x}) + \chi_1(\mathbf{x}) + \chi_2(\mathbf{x}) = 1, \forall \mathbf{x} \in X$. Here $\chi_1(\mathbf{x}) \equiv 1$, $\chi_2(\mathbf{x}) \equiv 1$ in a ball centered at $\mathbf{y}_1, \mathbf{y}_2$ with radius $r_0/2$ and are zeros outside the ball with radius r_0 respectively. $\chi_0(\mathbf{x}) = 1 - \chi_1(\mathbf{x}) - \chi_2(\mathbf{x})$. Denote

$$u(\mathbf{x}) = u(\mathbf{x})[\chi_0(\mathbf{x}) + \chi_1(\mathbf{x}) + \chi_2(\mathbf{x})] = u_0(\mathbf{x}) + u_1(\mathbf{x}) + u_2(\mathbf{x}).$$

We break the integral in (17) into three parts:

$$\int_X e^{i\tilde{k}\tilde{\phi}(\mathbf{x})} u(\mathbf{x}) d\mathbf{x} = \int_X e^{i\tilde{k}\tilde{\phi}(\mathbf{x})} (u_0(\mathbf{x}) + u_1(\mathbf{x}) + u_2(\mathbf{x})) d\mathbf{x} = \text{I+II+III}. \tag{29}$$

The first term can be reduced to Case 2. Now let's look at the second term in (29). We change the integration to the polar coordinates (r, θ, ψ) centered at $\mathbf{y}_1$ with $\theta \in [0, 2\pi]$ being the azimuthal angle, $\psi \in [0, \pi]$ being the polar angle and $\mathbf{y}_1 - \mathbf{y}_2$ being the polar axis. Then

$$\int_X e^{i\tilde{k}\tilde{\phi}(\mathbf{x})} u_1(\mathbf{x}) d\mathbf{x} = \int_0^{r_0} \int_{\partial B(\mathbf{y}_1, r)} e^{i\tilde{k}\tilde{\phi}(\mathbf{x})} u_1(\mathbf{x}) ds dr \tag{30}$$

It can be seen from (18) that $\nabla\tilde{\phi}(\mathbf{x}; \mathbf{y}_1, \mathbf{y}_2)$ is never aligned with the normal at $\mathbf{x}$ of the sphere centered at $\mathbf{y}_2$ except at the intersections of $l_{\mathbf{y}_1}^{\mathbf{y}_2}$ with the sphere. So on any

sphere $\partial B(\mathbf{y}_1, r)$, $\tilde{\phi}$ has exactly two stationary points at $\psi = 0$ and $\psi = \pi$ which are non-degenerate. At the two points,

$$
\begin{aligned}
&\tilde{\phi}(r,\theta,0) = 1 \\
&D_\perp^2 \tilde{\phi}(r,\theta,0) = \tfrac{-1}{r(r+|\mathbf{y}_1-\mathbf{y}_2|)} I_\perp \\
&u_1(r,\theta,0) = \tfrac{\chi_1(r,\theta,0)}{\|G_0(\cdot,\mathbf{y}_1)\|_2 \|G_0(\cdot,\mathbf{y}_2)\|_2 r(|\mathbf{y}_1-\mathbf{y}_2|+r)} \\
&\tilde{\phi}(r,\theta,\pi) = |\mathbf{y}_1-\mathbf{y}_2|^{-1}(2r-|\mathbf{y}_1-\mathbf{y}_2|) \\
&D_\perp^2 \tilde{\phi}(r,\theta,\pi) = \tfrac{|\mathbf{y}_1-\mathbf{y}_2|-2r}{r(|\mathbf{y}_1-\mathbf{y}_2|-r)} I_\perp \\
&u_1(r,\theta,\pi) = \tfrac{\chi_1(r,\theta,\pi)}{\|G_0(\cdot,\mathbf{y}_1)\|_2 \|G_0(\cdot,\mathbf{y}_2)\|_2 r(|\mathbf{y}_1-\mathbf{y}_2|-r)}
\end{aligned}
\tag{31}
$$

where $\perp$ denotes restriction to the tangent plane. Note that modulo a scaling factor r^{-1}, u_1 and its derivatives, and $D_\perp^2 \tilde{\phi}$ as functions on $\partial B(\mathbf{y}_1, r)$ are all smooth and uniformly bounded, i.e., $|D_\perp^\beta u_1| = O(r^{-1})$ and $\|D_\perp^2 \tilde{\phi}\| = O(r^{-1})$. After scaling $\partial B(\mathbf{y}_1, r)$ to the unit sphere and apply the stationary phase result (13) to the two stationary phase points, one gets

$$
\begin{aligned}
&\left| \int_{\partial B(\mathbf{y}_1,r)} e^{i\tilde{k}\tilde{\phi}(\mathbf{x})} u_1(\mathbf{x}) ds - \tfrac{2\pi i r^2 \tilde{k}^{-\frac{d-1}{2}}}{\|G_0(\cdot,\mathbf{y}_1)\|_2 \|G_0(\cdot,\mathbf{y}_2)\|_2} \left[-e^{i\tilde{k}} \chi_1(r,\theta,0) + \tfrac{e^{i\tilde{k}|\mathbf{y}_1-\mathbf{y}_2|^{-1}(2r-|\mathbf{y}_1-\mathbf{y}_2|)} \chi_1(r,\theta,\pi)}{|\mathbf{y}_1-\mathbf{y}_2|-2r} \right] \right| \\
&\lesssim \tilde{k}^{-\frac{d+1}{2}} r^2.
\end{aligned}
\tag{32}
$$

The righthand side in the above expression comes from an estimate of the righthand side term of the stationary phase formula (13) and the constant in $\lesssim$ is uniformly bounded when $r \to 0$. The first term in the square bracket is the leading term from the stationary phase at $\psi = 0$ on the sphere $\partial B(\mathbf{y}_1, r)$ and the phase is constant in r. The second term in the square bracket is the leading term from the stationary phase at $\psi = \pi$ on the sphere $\partial B(\mathbf{y}_1, r)$. However, it has a phase dependent on r which results in a higher order term after integration in r. Since all terms are integrable as $r \to 0$, we have

$$
\left| \int_X e^{i\tilde{k}\tilde{\phi}(\mathbf{x})} u_1(\mathbf{x}) d\mathbf{x} \right| = \left| \int_0^{r_0} \int_{\partial B(\mathbf{y}_1,r)} e^{i\tilde{k}\tilde{\phi}(\mathbf{x})} u_1(\mathbf{x}) ds dr \right| \lesssim \tilde{k}^{-\frac{d-1}{2}}. \tag{33}
$$

The third term in (29) can be shown in the same way.

In the special case that a source point locates on the boundary, e.g., $\mathbf{y}_1 \in \partial X$, one can easily modify the above argument to get the same estimate. The only difference is that integration is restricted to part of the sphere $\partial B(\mathbf{y}_1, r)$ for each fixed r in (33) in the polar coordinate decomposition. No matter which one of the two critical points, $\psi = 0$ or $\psi = \pi$,

is the point of stationary phase in $\partial B(\mathbf{y}_1, r) \cap X$, using one of the terms in (32), one gets the same estimate as in (33).

The constant in $\lesssim$ for this case comes from those estimates of the three terms on the righthand side of (29). The estimate of the first term is similar to case 2. The estimates for the last two terms come from the use of stationary phase lemma on the sphere $\partial B(\mathbf{y}_1, r)$ in (32). At the stationary points on each sphere, the value of u_1 only depends on $\|G_0(\cdot, \mathbf{y}_1)\|_2 \|G_0(\cdot, \mathbf{y}_2)\|_2$ due to the cancellation of the scaling factor r^2 after the integration in r. Again we reach the conclusion that the constant only depends on the relative positions of $\mathbf{y}_1, \mathbf{y}_2$ to X as well as on X.

From the above analysis, we see that the leading contribution to the correlation between two Green's functions, $| < \hat{G}_0(\cdot, \mathbf{y}_1), \hat{G}_0(\cdot, \mathbf{y}_2) >_X |$, comes from the stationary line $\tilde{l}^{\mathbf{y}_2}_{\mathbf{y}_1} \cap X$ or the boundary integral on ∂X after integration by part. All other cases can be reduced to the above three cases.

In 2D, the free space Green's function is of the form in (8) with the asymptotic formulas (9). For Case 1 and 2, the asymptotic formula (9) for $r \to \infty$ can be used as $k \to \infty$. For Case 3, the source singularity of the 2D Green's function is also integrable. So we have the following analogous results in 2D:

Case 1. Since the boundary ∂X is a one dimensional curve, there is some α, $1 \leq \alpha \leq \frac{d+1}{2} = \frac{3}{2}$, such that

$$\left| < \hat{G}_0(\cdot, \mathbf{y}_1), \hat{G}_0(\cdot, \mathbf{y}_2) > \right| \lesssim (k|\mathbf{y}_1 - \mathbf{y}_2|)^{-\alpha}, \quad \text{as } k|\mathbf{y}_1 - \mathbf{y}_2| \to \infty \tag{34}$$

Case 2. The leading contribution is due to the line of stationary phase $\tilde{l}^{\mathbf{y}_2}_{\mathbf{y}_1} \cap X$ except that the dimension orthogonal to the line is one, we have $\frac{d-1}{2} = \frac{1}{2}$ and

$$\left| < \hat{G}_0(\cdot, \mathbf{y}_1), \hat{G}_0(\cdot, \mathbf{y}_2) > \right| \lesssim (k|\mathbf{y}_1 - \mathbf{y}_2|)^{-\frac{1}{2}}, \text{ as } k|\mathbf{y}_1 - \mathbf{y}_2| \to \infty \tag{35}$$

Case 3. The singularity at the source point is integrable and

$$\left| < \hat{G}_0(\cdot, \mathbf{y}_1), \hat{G}_0(\cdot, \mathbf{y}_2) > \right| \lesssim (k|\mathbf{y}_1 - \mathbf{y}_2|)^{-\frac{1}{2}}, \text{ as } k|\mathbf{y}_1 - \mathbf{y}_2| \to \infty \tag{36}$$

□

Here we give a few remarks related to the theorem above.

Remark 2.1. *For $d = 3$, these results also hold for two unnormalized Green's functions, i.e., $| < G_0(\cdot, \mathbf{y}_1), G_0(\cdot, \mathbf{y}_2) >_X | \sim \left| < \hat{G}_0(\cdot, \mathbf{y}_1), \hat{G}_0(\cdot, \mathbf{y}_2) >_X \right|$, since there are two positive constants, c, C such that $0 < c < \|G_0(\cdot, \mathbf{y})\|_{2(X)} < C < \infty$ for a compact domain X as $k \to \infty$. However, this is not true for $d = 2$. If $\mathbf{y}_1, \mathbf{y}_2 \notin X$, $| < G_0(\cdot, \mathbf{y}_1), G_0(\cdot, \mathbf{y}_2) >_X | \sim k^{-\frac{1}{2}} \left| < \hat{G}_0(\cdot, \mathbf{y}_1), \hat{G}_0(\cdot, \mathbf{y}_2) >_X \right|$ as $k \to \infty$ due to the asymptotic formula (9).*

Remark 2.2. *One can also incorporate scaling factors into these estimates for the correlation between two Green's functions in Theorem 2.1. For example, the length scale of*

domain $X \in R^d$, denoted by L, can be easily scaled to $O(1)$ with a rescaled wave number Lk in the Helmholtz equation (3)*. A more interesting scaling factor is the ratio of the distance from the two sources $\mathbf{y}_i, i = 1, 2$ to X and the separation distance between the two sources, $|\mathbf{y}_1 - \mathbf{y}_2|$, when the ratio is large. Geometrically, this means that the difference between two distance functions, $|\mathbf{x} - \mathbf{y}_1| - |\mathbf{x} - \mathbf{y}_2|$, changes slowly with respect to $\mathbf{x} \in X$. Hence fast oscillations due to the rapid change of the phase function, $ik(|\mathbf{x} - \mathbf{y}_1| - |\mathbf{x} - \mathbf{y}_2|)$, is discounted and the decorrelation rate of two Green's functions is reduced.*

Assume that the size of X is $O(1)$ and $\frac{|\mathbf{y}_1-\mathbf{y}_2|}{dist(\mathbf{y}_1,X)} \sim \frac{|\mathbf{y}_1-\mathbf{y}_2|}{dist(\mathbf{y}_2,X)} \sim \rho \ll 1$, which falls into either Case 1 or Case 2 in Theorem 2.1. From (18)*, it is not hard to see that $\nabla\tilde{\phi}$ is scaled by ρ, $D^2\tilde{\phi}$ and $\det[D^2\tilde{\phi}]$ are scaled by ρ and ρ^d respectively when they are not degenerate, i.e., for a point $\mathbf{x} \in X \setminus \tilde{l}^{\mathbf{y}_2}_{\mathbf{y}_1}$. The scaling for $u(\mathbf{x})$ is canceled due to the normalization according to the definition* (15)*. For Case 1, the leading contribution for $\left| < \hat{G}_0(\cdot, \mathbf{y}_1), \hat{G}_0(\cdot, \mathbf{y}_2) > \right|$ comes from the last term in* (20)*. Since $X \cap \tilde{l}^{\mathbf{y}_2}_{\mathbf{y}_1} = \emptyset$, both $\nabla\tilde{\phi}$ and $D^2\tilde{\phi}$ are not degenerate on ∂X. A scaling factor of ρ^{-1} due to $\nabla\tilde{\phi}$ in the integrand scales the factor $\tilde{k}^{-1}$ in front of the boundary integral to $(\rho\tilde{k})^{-1}$. In a generic case in which $\nabla\phi$ vanishes tangential to the boundary on ∂X at isolated stationary points, the scaling factor of $\rho^{-\frac{d-1}{2}}$ from $det[D^2_\perp\tilde{\phi}]$ scales $\tilde{k}$ to $\rho\tilde{k}$ when applying the stationary phase Lemma to the integration on ∂X at stationary points. In other words, $\tilde{k}$ is rescaled to $\rho\tilde{k}$ for Case 1. For Case 2 in Theorem 2.1, in which $X \cap \tilde{l}^{\mathbf{y}_2}_{\mathbf{y}_1} \neq \emptyset$, the leading contribution for $\left| < \hat{G}_0(\cdot, \mathbf{y}_1), \hat{G}_0(\cdot, \mathbf{y}_2) > \right|$ comes from the line of stationary phase in a generic situation (see* (25)*). In this case, $D\tilde{\phi}$ and $D^2\tilde{\phi}$ are degenerate on the line of stationary phase, along which $D^2_\perp\tilde{\phi}$ and $\det[D^2_\perp\tilde{\phi}]$ are scaled by ρ^2 and $\rho^{2(d-1)}$ respectively from* (19)*. Applying the stationary phase result, Lemma 2.1, in the plane perpendicular to the line of stationary phase, $\tilde{k}$ is rescaled to $\rho^2\tilde{k}$, which is the parabolic scaling. For both cases we see that $\tilde{k}$ is at least rescaled to $\rho\tilde{k}$ in the estimate of the correlation between two Green's functions of the Helmholtz equation in the high frequency limit.*

Remark 2.3. *One can extend the arguments and results in Theorem 2.1 to more general situations. For example, X is a compact manifold embedded in R^d with $\dim(X) = s < d$, such as a surface ($s = 2$) in R^3 or a curve ($s = 1$) in $R^d, d = 2, 3$. If X is a compact manifold without boundary, e.g., a closed surface or curve, for two points $\mathbf{y}_1, \mathbf{y}_2 \notin X$, there is some α, $0 \leq \alpha \leq \frac{s}{2}$*

$$\left| < \hat{G}_0(\cdot, \mathbf{y}_1), \hat{G}_0(\cdot, \mathbf{y}_2) > \right| \lesssim (k|\mathbf{y}_1 - \mathbf{y}_2|)^{-\alpha}, \quad \text{as } k|\mathbf{y}_1 - \mathbf{y}_2| \to \infty. \tag{37}$$

The two extreme cases are: (1) $\alpha = 0$ happens when a piece of X stays on a level set of the phase function $\tilde{\phi}(\mathbf{x}) = |\mathbf{y}_1 - \mathbf{y}_2|^{-1}(|\mathbf{x} - \mathbf{y}_1| - |\mathbf{x} - \mathbf{y}_2|)$; (2) $\alpha = \frac{s}{2}$ happens when the phase function $\tilde{\phi}(\mathbf{x})$ has isolated non-degenerate stationary points on X, e.g., $X \cap \tilde{l}^{\mathbf{y}_2}_{\mathbf{y}_1} \neq \emptyset$. If X is a compact manifold with boundary, there is some α, $0 \leq \alpha \leq \frac{s+1}{2}$ such that

$$\left| < \hat{G}_0(\cdot, \mathbf{y}_1), \hat{G}_0(\cdot, \mathbf{y}_2) > \right| \lesssim (k|\mathbf{y}_1 - \mathbf{y}_2|)^{-\alpha}, \quad \text{as } k|\mathbf{y}_1 - \mathbf{y}_2| \to \infty. \tag{38}$$

The two extreme cases are: (1) $\alpha = 0$ happens when a piece of X stays on a level set of the phase function $\tilde{\phi}(\mathbf{x})$; (2) $\alpha = \frac{s+1}{2}$ happens if the phase function $\tilde{\phi}(\mathbf{x})$ has no stationary poiny in the interior of X and has non-degenerate isolated stationary points on ∂X. If there are isolated non-degenerate stationary points in the interior of X, e.g., $X \cap \tilde{l}_{\mathbf{y}_1}^{\mathbf{y}_2} \neq \emptyset$, $\alpha = \frac{s}{2}$.

Figure 3 shows typical scenarios for $\alpha = \frac{s}{2}$. The ray going through $\mathbf{y}_1, \mathbf{y}_2$ intersects X transversally at a finite number of isolated points. Those intersections are isolated non-degenerate stationary points in X.

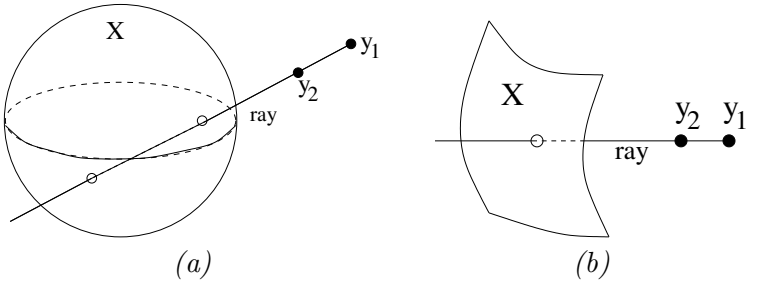

FIGURE 3. X is an embedded manifold

Remark 2.4. *According to the Hessian estimate* (19)*, there are two axi-symmetric k dependent domains around the stationary line $\tilde{l}_{\mathbf{y}_1}^{\mathbf{y}_2}$ on each side of $\mathbf{y}_1$ and $\mathbf{y}_2$, denoted by R_1 and R_2 respectively (see Figure 4), in which the phase function $\tilde{k}\tilde{\phi}$ does not change rapidly due to the smallness of $|\nabla\tilde{\phi}|$ which is $\lesssim \tilde{k}^{-1}$ in these k dependent domains. For example, let's look at a point $\mathbf{x} \in \tilde{l}_{\mathbf{y}_1}^{\mathbf{y}_2}$ on the side of $\mathbf{y}_2$ and denote $r = \pm|\mathbf{x} - \mathbf{y}_2|$. Again we use the coordinate system $\mathbf{x}$=(r, ξ, η) as shown in Figure 4. Since $\tilde{\phi}(r, 0, 0)$=1, $|\nabla\tilde{\phi}(r, 0, 0)|$=0, $r>0$, for a point (r, ξ, η) with $r > 0$, $\sqrt{\xi^2 + \eta^2} \lesssim \frac{r(r+|\mathbf{y}_1-\mathbf{y}_2|)}{k|\mathbf{y}_1-\mathbf{y}_2|}$, from* (19) *we have*

$$\tilde{k}|\nabla\tilde{\phi}(r, \xi, \eta)| \lesssim \frac{k|\mathbf{y}_1 - \mathbf{y}_2|\sqrt{\xi^2 + \eta^2}}{r(r + |\mathbf{y}_1 - \mathbf{y}_2|)} \lesssim 1. \tag{39}$$

Hence $< \hat{G}_0(\cdot, \mathbf{y}_1), \hat{G}_0(\cdot, \mathbf{y}_2) >$ is not an oscillatory integral in R_1 or R_2 and the two Green's functions do not decorrelate fast in these two domains. We will provide more special k dependent setups of domains X, Y such that $G(\mathbf{x}, \mathbf{y}_1)$ and $G(\mathbf{x}, \mathbf{y}_2)$ do not decorrelate fast in X for two sources $\mathbf{y}_1, \mathbf{y}_2 \in Y$ in Section 4.2.

Remark 2.5. *The correlation between two Green's functions is of importance in the resolution study of imaging systems. The resolution of an imaging system is defined as the minimal separation distance between two point scatterers that the system can distinguish. Hence the image resolution can be characterized by the decorrelation length between two Green's functions. The faster the decorrelation, the finer the resolution is. Suppose X is a compact planar region in R^3 where the wave field is measured, i.e., a mirror made of transducers. The wave field observed on X corresponding to a point source*

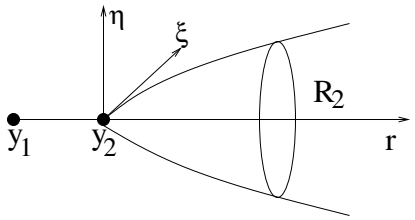

FIGURE 4. A domain where two Green's functions do not decorrelate fast.

(or a point scatterer) can be approximated by the Green's function. If two point sources, $\mathbf{y}_1, \mathbf{y}_2$*, are separated in the range direction, i.e., the line connecting* $\mathbf{y}_1$ *and* $\mathbf{y}_2$ *intersects* X *orthogonally,* $|< G_0(\cdot, \mathbf{y}_1), G_0(\cdot, \mathbf{y}_2) >| \sim O((k|\mathbf{y}_1 - \mathbf{y}_2|)^{-\frac{1}{2}})$*, since the intersection point is a point of stationary phase. While if two point sources,* $\mathbf{y}_1, \mathbf{y}_2$*, are separated in the cross range direction, i.e., the line connecting* $\mathbf{y}_1$ *and* $\mathbf{y}_2$ *is parallel to* X*, we have* $|< G_0(\cdot, \mathbf{y}_1), G_0(\cdot, \mathbf{y}_2) >| \sim O((k|\mathbf{y}_1 - \mathbf{y}_2|)^{-\frac{3}{2}})$*, since there is no point of stationary phase. Hence it shows the well-known fact that cross range resolution is higher than range resolution for a typical imaging system.*

2.2. **Correlation between two Green's functions in the high frequency limit in heterogeneous media.** In a heterogeneous medium, the correlation between two Green's functions is similar to that in a homogeneous medium in the high frequency limit. We provide the arguments for the results in Theorem 2.1 in a heterogeneous medium based on the validity of geometric optics Ansatz [21, 3]. A geometric optics Ansatz for the Green's functions of the Helmholtz equation takes the form

$$G(\mathbf{x}, \mathbf{y}) = e^{ik\phi(\mathbf{x},\mathbf{y})} \sum_{m=0}^{M} a_m(\mathbf{x}, \mathbf{y}) k^{-m} + O(k^{-M-1}), \quad \text{as } k \to \infty, \tag{40}$$

where $\phi(\mathbf{x}, \mathbf{y})$ is the phase function and $a_m(\mathbf{x}, \mathbf{y})$ are the amplitude functions, and satisfies the following conditions at the source point $\mathbf{y}$:

$$\lim_{\mathbf{x}\to\mathbf{y}} \left(\frac{\phi(\mathbf{x}, \mathbf{y})}{|\mathbf{x} - \mathbf{y}|} - n(\mathbf{y}) \right) = 0, \quad \lim_{\mathbf{x}\to\mathbf{y}} a_0(\mathbf{x}, \mathbf{y}) 4\pi |\mathbf{x} - \mathbf{y}| = 1. \tag{41}$$

The phase function can be prescribed by a Hamiltonian system with the Hamiltonian $H(\mathbf{x}, \mathbf{p}) = |\mathbf{p}| - n(\mathbf{x})$ and $\mathbf{p} = \nabla\phi$. The bicharacteristics $(\mathbf{x}(t), \mathbf{p}(t))$ and the phase function satisfy the following ordinary differential equations (ODE) in the phase space.

$$\begin{aligned}
&\frac{d\mathbf{x}(t, \mathbf{x}_0, \mathbf{p}_0)}{dt} = \nabla_{\mathbf{p}} H(\mathbf{x}, \mathbf{p}) = \frac{\mathbf{p}}{n(\mathbf{x})}, \qquad \mathbf{x}(0) = \mathbf{x}_0, \\
&\frac{d\mathbf{p}(t, \mathbf{x}_0, \mathbf{p}_0)}{dt} = -\nabla_{\mathbf{x}} H(\mathbf{x}, \mathbf{p}) = \nabla n(\mathbf{x}), \quad \mathbf{p}(0) = \mathbf{p}_0 = \nabla\phi(\mathbf{x}_0) \\
&\frac{d\phi(\mathbf{x}(t, \mathbf{x}_0, \mathbf{p}_0))}{dt} = \nabla\phi \cdot \frac{d\mathbf{x}}{dt} = n(\mathbf{x}), \qquad \phi(0) = \phi(\mathbf{x}_0)
\end{aligned} \tag{42}$$

The projection of the bicharacteristics in the physical space, i.e., $\mathbf{x}(t, \mathbf{y}_0, \mathbf{p}_0)$, are called rays. Each ray is a geodesic in the physical space with the index of refraction $n(x) = \frac{1}{c(\mathbf{x})}$ as the metric, where $c(\mathbf{x})$ is the wave speed. $|\phi(\mathbf{x}(t_2, \mathbf{x}_0, \mathbf{p}_0)) - \phi(\mathbf{x}(t_1, \mathbf{x}_0, \mathbf{p}_0))|$ is the shortest travel time or geodesic distance between points $\mathbf{x}(t_1, \mathbf{x}_0, \mathbf{p}_0)$ and $\mathbf{x}(t_2, \mathbf{x}_0, \mathbf{p}_0)$.

For the Green's function with a point source at $\mathbf{y}_0$, rays $\mathbf{x}(t, \mathbf{y}_0, \hat{\theta})$ are emanating from the source $\mathbf{y}_0$ in all directions and can be parameterized by the initial directions, i.e., the take-off angles $\hat{\theta} \in S^{d-1}$ on a unit sphere. The ODEs for the rays (42) have initial conditions $\mathbf{x}(0, \mathbf{y}_0, \hat{\theta}) = \mathbf{y}_0, \mathbf{p}(0, \mathbf{y}_0, \hat{\theta}) = n(\mathbf{y}_0)\hat{\theta}, \phi(0, \mathbf{y}_0, \hat{\theta}) = 0$, with $a_0(0, \hat{\theta})$ evenly distributed in all $\hat{\theta}$. If there is no crossing of rays in the physical space, every point $\mathbf{x}$ has a unique ray passing through it, i.e., $\forall \mathbf{x}, \exists! t(\mathbf{x}), \hat{\theta}(\mathbf{x})$ such that $\mathbf{x}(t(\mathbf{x}), \mathbf{y}_0, \hat{\theta}(\mathbf{x})) = \mathbf{x}$. Moreover, the ray connecting $\mathbf{y}_0$ and $\mathbf{x}$ is the geodesic and the phase function $\phi(\mathbf{x}, \mathbf{y}_0)$ is the geodesic distance or the shortest travel time between these two points.

Theorem 2.2. *If two Green's functions with source points $\mathbf{y}_1, \mathbf{y}_2$ can be approximated by the following geometric optics Ansatz*

$$\left| G(\mathbf{x}, \mathbf{y}_j) - e^{ik\phi(\mathbf{x}, \mathbf{y}_j)} A_j(\mathbf{x}) \right| \lesssim k^{-(M+1)}, \quad j = 1, 2, \tag{43}$$

for some integer $M > 0$ and functions ϕ, A_j that satisfy (41) *and are smooth away from the sources, then the estimates in Theorem 2.1 holds.*

Proof. Since

$$\left| < \hat{G}(\cdot, \mathbf{y}_1), \hat{G}(\cdot, \mathbf{y}_2) > - \int_X e^{i\tilde{k}\tilde{\phi}(\mathbf{x})} u(\mathbf{x}) d\mathbf{x} \right| \lesssim k^{-(M+1)}, \tag{44}$$

where

$$\tilde{k} = k\phi(\mathbf{y}_1, \mathbf{y}_2), \quad \tilde{\phi}(\mathbf{x}) = \phi^{-1}(\mathbf{y}_1, \mathbf{y}_2)(\phi(\mathbf{x}, \mathbf{y}_1) - \phi(\mathbf{x}, \mathbf{y}_2)), \quad u(\mathbf{x}) = \frac{A_1(\mathbf{x}) A_2(\mathbf{x})}{\|G(\cdot, \mathbf{y}_1)\|_2 \|G(\cdot, \mathbf{y}_2)\|_2},$$

one only needs to estimate $|\int_X e^{i\tilde{k}\tilde{\phi}(\mathbf{x})} u(\mathbf{x}) d\mathbf{x}|$. Let $\Gamma_{\mathbf{y}_1}^{\mathbf{y}_2}$ be the unique ray that passes through $\mathbf{y}_1$ and $\mathbf{y}_2$ as illustrated in Figure 5 (a). If $n(\mathbf{x})$ is smooth and $0 < c \le n(\mathbf{x}) \le C < \infty$, one has (see Figure 5(b))

$$c|\mathbf{y}_1 - \mathbf{y}_2| \le \phi(\mathbf{y}_1, \mathbf{y}_2) \le C|\mathbf{y}_1 - \mathbf{y}_2|, \quad |\phi(\mathbf{x}, \mathbf{y}_1) - \phi(\mathbf{x}, \mathbf{y}_2)| \le \phi(\mathbf{y}_2, \mathbf{y}_1). \tag{45}$$

So the phase function $\tilde{\phi}(\mathbf{x})$ attains the global maximum or minimum ± 1 on the part of the ray $\Gamma_{\mathbf{y}_1}^{\mathbf{y}_2}$ which is outside the interval between $\mathbf{y}_1$ and $\mathbf{y}_2$, denoted by $\tilde{\Gamma}_{\mathbf{y}_1}^{\mathbf{y}_2}$. Moreover, $\nabla_{\mathbf{x}}\phi(\mathbf{x}, \mathbf{y}_1) - \nabla_{\mathbf{x}}\phi(\mathbf{x}, \mathbf{y}_2) \neq 0, \forall \mathbf{x} \notin \tilde{\Gamma}_{\mathbf{y}_1}^{\mathbf{y}_2}$ because the two different and unique geodesics connecting $\mathbf{x}, \mathbf{y}_1$ and $\mathbf{x}, \mathbf{y}_2$ respectively can not be tangent to each other at $\mathbf{x}$. So $\tilde{\Gamma}_{\mathbf{y}_1}^{\mathbf{y}_2}$ is a stationary curve in the heterogeneous medium and plays the same role as the stationary line $\tilde{l}_{\mathbf{y}_1}^{\mathbf{y}_2}$ in a homogeneous medium. For those various cases proved in Theorem 2.1, $M+1 \ge 2 \ge \alpha$, we get the same results as those in Theorem 2.1 since $k\phi(\mathbf{y}_1, \mathbf{y}_2) \sim k|\mathbf{y}_1 - \mathbf{y}_2|$ from (45). This is true when $\mathbf{y}_1$ and/or $\mathbf{y}_2$ are in X as well since the amplitude satisfying (41) has the same type of source singularity as that in the free space Green's function $G_0(\mathbf{x}, \mathbf{y})$. □

Remark 2.6. *More general scenarios as discussed in Remark 2.3, i.e., X is a manifold embedded in R^d, can also be extended to heterogeneous media as long as the geometric optics Ansatz holds.*

There are possible complications for geometric optics Ansatz in heterogeneous medium due to crossing of rays or formation of caustics. In those situations the phase and the amplitude can no longer be defined as global smooth functions in physical space. However, bicharacteristics in phase space are still well defined and smooth. In the case that there is a finite number of rays connecting $\mathbf{y}_1, \mathbf{y}_2$ and there is a partition of unity in the angular domain for the takeoff angles $\hat{\theta}$ on S^{d-1} such that there is a small angular cone around each ray such that the rays in each cone do no cross each other in X, one can apply the above arguments to the wave field corresponding to each cone and superpose the partition of unity in angular space to get those same results.

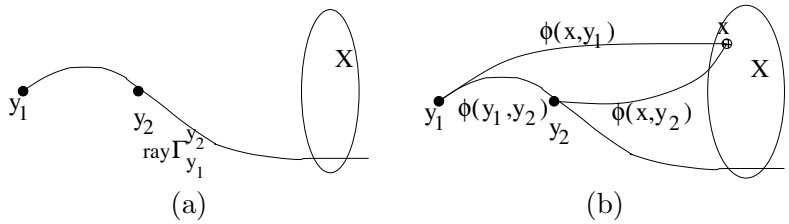

FIGURE 5. Rays in inhomogeneous medium

3. Approximate Separability Estimates for the Green's Functions of the Helmholtz equation in the High Frequency Limit

In this section we present the estimates for both lower and upper bounds for the approximate separability for the Green's functions of the Helmholtz equation in the high frequency limit. First we introduce some background and a few definitions for the approximation of a set of vectors by the best linear subspace with a given dimension in 2-norm, which are extended later to the approximation of a family of functions by a linear subspace in a function space equipped with L_2 norm.

3.1. Approximating a set of almost orthogonal vectors by a linear space.

Let $\mathbf{v}_m \in R^d, m = 1, 2, \ldots, N$ be a set of vectors. Define matrix $V = [\mathbf{v}_1, \mathbf{v}_2, \ldots, \mathbf{v}_N]$ and matrix $A = [a_{mn}]_{N\times N} = V^T V$. Let $\lambda_1 \geq \lambda_2 \geq \ldots \geq \lambda_N \geq 0$ be the eigenvalues of A, then $tr(A) = \sum_{m=1}^N \lambda_m = \sum_m^N \|\mathbf{v}_m\|_2^2$. $\sqrt{\lambda_1} \geq \sqrt{\lambda_2} \geq \ldots \geq \sqrt{\lambda_N} \geq 0$ are also called the singular values of V. The best linear subspace, denoted by $\overline{S}_l$, of all linear subspaces of dimension l, denoted by S_l, that approximates the set of vectors $\{\mathbf{v}_m\}_{m=1}^N$ in least squares sense is the space spanned by the first l left singular vectors of V and satisfies

$$\sum_m^N \|\mathbf{v}_m - P_{\overline{S}_l}\mathbf{v}_m\|_2^2 = \min_{S_l, \dim(S)=l} \sum_m^N \|\mathbf{v}_m - P_{S_l}\mathbf{v}_m\|_2^2 = \sum_{m=l+1}^N \lambda_m, \tag{46}$$

where $P_{S_l}\mathbf{v}$ denotes the projection of $\mathbf{v}$ in S_l. In other words,

$$\lambda_l = \max_{\hat{\mathbf{e}}\in R^d, \|\hat{\mathbf{e}}\|_2=1, \hat{\mathbf{e}}\perp \overline{S}_{l-1}} \sum_j^N |\mathbf{v}_j \cdot \hat{\mathbf{e}}|^2, \tag{47}$$

is the maximum reduction of approximation error in term of least squares for the set of vectors $\{\mathbf{v}_m\}_{m=1}^N$ when adding one more dimension to the previous optimal $l-1$ dimensional linear subspace. Here we introduce two definitions for approximate rank estimates for a symmetric non-negative matrix A with ϵ tolerance in 2-norm.

Definition 3.1. *Given* $\epsilon > 0$, $\overline{N}^\epsilon = \max_{1\le m\le N} m$, *s.t.* $\sqrt{\lambda_m} \ge \epsilon$, *i.e.,*$\overline{N}^\epsilon$ *denotes the largest* m *such that* $\sqrt{\lambda_m} \ge \epsilon$.

Definition 3.2. *Given* $1 \ge \epsilon > 0$, $\underline{N}^\epsilon = \min M$, *s.t.* $\sum_{m=M+1}^N \lambda_m \le \epsilon^2 \sum_{m=1}^N \lambda_m$.

If $A = V^T V$, Definition 3.2 implies that if a linear subspace S^ϵ satisfies

$$\frac{\sum_{m=1}^N \|\mathbf{v}_m - P_{S^\epsilon}\mathbf{v}_m\|_2^2}{\sum_{m=1}^N \|\mathbf{v}_m\|_2^2} \le \epsilon^2 \tag{48}$$

then $\dim(S^\epsilon) \ge \underline{N}^\epsilon$. Assume $0 < c \le \|\mathbf{v}_m\|_2 \le C < \infty, m = 1, 2, \ldots, N$, if a linear subspace S^ϵ satisfies

$$\sqrt{\frac{\sum_{m=1}^N \|\mathbf{v}_m - P_{S^\epsilon}\mathbf{v}_m\|_2^2}{N}} \le c\epsilon,$$

which implies

$$\frac{\sum_{m}^N \|\mathbf{v}_m - P_{S^\epsilon}\mathbf{v}_m\|_2^2}{\sum_{m=1}^N \|\mathbf{v}_m\|_2^2} \le \epsilon^2,$$

then we can conclude $\dim(S^\epsilon) \ge \underline{N}^\epsilon$. In other words, the least dimension of a linear subspace that has an $c\epsilon$-r.m.s. (root mean square) approximation of a set of vectors $\mathbf{v}_m, m = 1, 2, \ldots, N$ is at least N^ϵ. The root mean square approximation will lead to the lower bound estimate of L_2 approximate separability for the Green's function in the continuous case.

In the previous section, we proved a fast decorrelation between two Green's functions of the Helmholtz equation in the high frequency limit:

$$| < \hat{G}(\cdot, \mathbf{y}_1), \hat{G}(\cdot, \mathbf{y}_1) > | \lesssim (k|\mathbf{y}_1 - \mathbf{y}_2|)^{-\alpha}$$

for some $\alpha > 0$ as $k|\mathbf{y}_1 - \mathbf{y}_2| \to \infty$. Geometrically it means that two Green's functions with sources separated a little more than one wavelength, e.g., $|\mathbf{y}_1 - \mathbf{y}_2| = k^{-1+\delta}$ for any small $\delta > 0$, become almost orthogonal to each other as $k \to \infty$. Intuitively, for two domains $X, Y \subset R^d$, if one views $G(\mathbf{x}, \mathbf{y})$ as a family of functions in $L_2(X)$ parameterized by $\mathbf{y} \in Y$ and lays down a grid $\mathbf{y}_j \in Y$ with a grid size $h = k^{-1+\delta}$ for any small $\delta > 0$, $G(\mathbf{x}, \mathbf{y}_j)$ is a set of almost orthogonal vectors in $L_2(X)$. This leads naturally to a question in linear algebra: what is the least dimension of a linear space that can contain a set of almost orthogonal vectors. This question was studied in [1] for a set of almost orthogonal unit vectors, $\mathbf{v}_m \in R^d$, $m = 1, 2, \ldots, N$, $|\mathbf{v}_m^T \mathbf{v}_n| \le \epsilon$, $m \ne n$. Denote $V = [\mathbf{v}_1, \mathbf{v}_2, \ldots, \mathbf{v}_N]$. A

rank estimate for the matrix V^TV, which is a small perturbation of an identity matrix in the off-diagonals, was proved. In particular, the asymptotic estimate for $\frac{1}{\sqrt{N}} < \epsilon \leq \frac{1}{2}$ is optimal and was used to show the sharpness of Johnson-Lindenstraus Lemma [20]. However, this result can not address our problem adequately for the following two reasons. First, the pairwise almost orthogonality assumption in [1] is the same for any pair of vectors. In our problem, a family of Green's functions parameterized by their source locations have spatial structures, i.e., the angle between two Green's functions depends on the separation distance of the two sources. The spatial structure has to be taken into account to get the right scaling to get a sharp estimate. Second, a family of Green's functions $G(\mathbf{x}, \mathbf{y}) \in L_2(X)$ parameterized by the sources $\mathbf{y} \in Y$ can not be contained in a finite dimensional linear subspace in $L_2(X)$ if Y is a compact domain with positive measure. The approximate separability means that one needs to estimate the least dimension of a linear subspace that can approximate a set of vectors to a certain tolerance. In Lemma 3.1, we first develop a sharp rank estimate for a discrete set of Green's functions of the Helmholtz equation in the high frequency limit by taking into account both the spatial distribution of the sources and the approximation tolerance. Based on the lemma we will prove lower bound estimates for the approximate separability of the Green's functions for Helmholtz equation in the high frequency limit.

Let $G_0(\mathbf{x}, \mathbf{y}), \mathbf{x} \in X, \mathbf{y} \in Y$ be the free space Green's function of the Helmholtz equation (3) and $\hat{G}_0(\cdot, \mathbf{y})$ be its normalized version in $L_2(X)$. Our results are based on the fast decorrelation of the Green's functions of the Helmholtz equation in the high frequency limit. X, Y are two compact smooth manifolds embedded in R^d, i.e., either of them may be a compact domain in $R^d, d = 2, 3$, or a compact surface embedded in R^3 or a compact curve embedded in $R^d, d = 2$ or 3. Without loss of generality, we assume $d \geq \dim(X) \geq \dim(Y) = s$. For a smooth compact manifold Y with $\dim(Y) = s = 1, 2, 3$, there exists a piece of $O(1)$ size which is diffeomorphic to a one dimensional unit interval, a two dimensional unit square or a three dimensional unit cube respectively. Moreover, the diffeomorphism has a bounded metric distortion. So in the following proofs we only consider Y to be a unit interval, a unit square or a unit cube for simplicity. The following Lemma 3.1 shows the lower bound estimates for the dimension of a linear subspace in $L_2(X)$ that approximates a set of Green's function $\hat{G}_0(\cdot, \mathbf{y}_m)$ with ϵ-r.m.s error with $\mathbf{y}_m$ properly sampled in Y.

Lemma 3.1. *Let X, Y be two compact manifolds embedded in $R^d, d = 2, 3$ and $d \geq \dim(X) \geq \dim(Y) = s$. If there is a $\alpha > 0$ such that for any two points $\mathbf{y}_1, \mathbf{y}_2 \in Y$,*

$$| < \hat{G}_0(\cdot, \mathbf{y}_1), \hat{G}_0(\cdot, \mathbf{y}_2) >_X | \lesssim (k|\mathbf{y}_1 - \mathbf{y}_2|)^{-\alpha} \quad \text{as } k|\mathbf{y}_1 - \mathbf{y}_2| \to \infty, \tag{49}$$

then for any $\delta > 0$ arbitrary close to 0, there are points $\mathbf{y}_m \in Y, m = 1, 2, \ldots, N_\delta^s \sim k^{s-\delta}$, such that the matrix $A =< \hat{G}_0(\cdot, \mathbf{y}_m), \hat{G}_0(\cdot, \mathbf{y}_n) >_X$ satisfies

$$\underline{N}_k^\epsilon \gtrsim \begin{cases} (1-\epsilon^2)^2 k^{2\alpha}, & \alpha < \frac{s}{2}, \\ (1-\epsilon^2)^2 k^{s-\delta}, & \alpha \geq \frac{s}{2}, \end{cases} \tag{50}$$

and

$$\overline{N}_k^\epsilon \lesssim \begin{cases} \epsilon^{-4} k^{2(s-\alpha-\delta)}, & \alpha < \frac{s}{2}, \\ \epsilon^{-4} k^{s-\delta}, & \alpha \geq \frac{s}{2}, \end{cases} \tag{51}$$

for k large enough, where the constants in $\lesssim$ and $\gtrsim$ depend on X, Y and the distance in-between.

Proof. We prove the statement for $X, Y \subset R^3$ and $\dim(Y) = s = 1, 2, 3$ respectively. Without loss of generality, we consider Y to be a unit interval, a unit square or a unit cube respectively. The case for $X, Y \subset R^2$ can be proved in exactly the same way.

Case 1: $s = 1$, Y is a line segment of unit length in R^3. Let $\mathbf{y}_m$ be the grid points of a uniform grid in Y (Figure 6(a)) with grid size $h = k^{\delta-1}$, $0 < \delta < 1$ such that $|\mathbf{y}_m - \mathbf{y}_n| = |m-n|h,\ m, n = 1, 2, \ldots, n_k^h = k^{1-\delta}$. The matrix

$$A = (a_{mn})_{n_k^h \times n_k^h}, \quad a_{mn} = < \hat{G}_0(\cdot, \mathbf{y}_m), \hat{G}_0(\cdot, \mathbf{y}_n) >_X, \tag{52}$$

has the following properties

$$a_{mm} = 1, \quad |a_{mn}| \lesssim |m-n|^{-\alpha} k^{-\alpha\delta}, \quad m, n = 1, 2, \ldots, n_k^h. \tag{53}$$

Let $\lambda_1 \geq \lambda_2 \geq \ldots \geq \lambda_{n_k^h} \geq 0$ be the eigenvalues of A. Then $\sum_{m=1}^{n_k^h} \lambda_m = n_k^h$. Since $\overline{N}_k^\epsilon = \max_{1 \leq m \leq n_k^h} m,\ s.t.\ \sqrt{\lambda_m} \geq \epsilon$ and $\underline{N}_k^\epsilon = \min M,\ s.t.\ \sum_{m=M+1}^{n_k^h} \lambda_m \leq \epsilon^2 \sum_{m=1}^{n_k^h} \lambda_m = \epsilon^2 n_k^h$, we have

$$\sum_{m=1}^{\underline{N}_k^\epsilon} \lambda_m \geq (1-\epsilon^2) \sum_{m=1}^{n_k^h} \lambda_m = (1-\epsilon^2) n_k^h$$

and

$$\sum_{m=1}^{n_k^h} \lambda_m^2 > \sum_{m=1}^{\underline{N}_k^\epsilon} \lambda_m^2 \geq \underline{N}_k^\epsilon \left[\frac{(1-\epsilon^2) n_k^h}{\underline{N}_k^\epsilon} \right]^2 = \frac{[(1-\epsilon^2) n_k^h]^2}{\underline{N}_k^\epsilon}, \tag{54}$$

and

$$\sum_{m=1}^{n_k^h} \lambda_m^2 > \sum_{m=1}^{\overline{N}_k^\epsilon} \lambda_m^2 \geq \overline{N}_k^\epsilon \epsilon^4. \tag{55}$$

At the same time, for a fixed $\alpha > 0$ and take $0 < \delta < 1$ arbitrary close to 0,

$$\begin{aligned}
&\textstyle\sum_{m=1}^{n_k^h} \lambda_m^2 = tr(A^T A) = \sum_{m=1}^{n_k^h} \sum_{n=1}^{n_k^h} a_{mn}^2 \\
&= \textstyle\sum_{m=1}^{n_k^h} a_{mm}^2 + 2\sum_{n=1}^{n_k^h-1} \sum_{m=n+1}^{n_k^h} a_{m,m-n}^2 \\
&\lesssim n_k^h + 2\textstyle\sum_{n=1}^{n_k^h-1} (n_k^h - n) n^{-2\alpha} k^{-2\alpha\delta} \qquad (56)\\
&\lesssim \begin{cases} k^{1-\delta} + k^{2(1-\delta-\alpha)} \lesssim k^{2(1-\delta-\alpha)}, & \alpha < \frac{1}{2},\ 2\alpha < 1-\delta < 1 \\ k^{1-\delta} + k^{1-2\delta} \ln k \lesssim k^{1-\delta}, & \alpha = \frac{1}{2},\ 0 < \delta < 1 \\ k^{1-\delta} + k^{1-\delta-2\alpha\delta} \lesssim k^{1-\delta}, & \alpha > \frac{1}{2},\ 0 < \delta < 1 \end{cases}
\end{aligned}$$

Hence for a fixed $\alpha > 0$ and any $0 < \delta < 1$ arbitrary close to 0, combining (54) and (56) we have

$$\underline{N}_k^\epsilon \gtrsim \begin{cases} (1-\epsilon^2)^2 k^{2\alpha}, & \alpha < \frac{1}{2} \\ (1-\epsilon^2)^2 k^{1-\delta}, & \alpha \geq \frac{1}{2} \end{cases}, \qquad (57)$$

and combining (55) and (56) we have

$$\overline{N}_k^\epsilon \lesssim \begin{cases} \epsilon^{-4} k^{2(1-\alpha-\delta)}, & \alpha < \frac{1}{2} \\ \epsilon^{-4} k^{1-\delta}, & \alpha \geq \frac{1}{2} \end{cases}. \qquad (58)$$

Case 2: $s = 2$, Y is a unit square in R^3. Let $\mathbf{y}_m, m = 1, 2, \ldots, n_k^h = k^{2(1-\delta)}$ be the grid points of an uniform grid in Y with a grid size $h = k^{\delta-1}, 0 < \delta < 1$ (see Figure 6(b)). Define matrix A as in (52). Let $\lambda_1 \geq \lambda_2 \geq \ldots \geq \lambda_{n_k^h} \geq 0$ be its eigenvalues, then $\sum_{m=1}^{n_k^h} \lambda_m = n_k^h$ and we have (54), (55). At the same time

$$\sum_{m=1}^{n_k^h} \lambda_m^2 = tr(A^T A) = \sum_{m=1}^{n_k^h} \sum_{n=1}^{n_k^h} a_{mn}^2. \qquad (59)$$

We look at the sum of each row. Assume $\mathbf{y}_m$ is the center of the square. We divide all other points into groups of 1st square neighbors, 2nd square neighbors, ..., j-th square neighbors, denoted by $S_j, j = 1, 2, \ldots, J \sim h^{-1} = k^{1-\delta}$. See Figure 6(b). S_j contains those $4(2j+1) - 4 = 8j$ grid points that are on the 4 sides of the square centered at $\mathbf{y}_m$ with each side of length $2jh$. We have $jh \leq |\mathbf{y}_{n_j} - \mathbf{y}_m| \leq \sqrt{2} jh, \mathbf{y}_{n_j} \in S_j$, and hence $a_{m,n_j} \lesssim (kjh)^{-\alpha} = j^{-\alpha} k^{-\alpha\delta}$. For a fixed $\alpha > 0$ and take $0 < \delta < 1$ arbitrary close to 0, we

get

$$\sum_{n=1}^{n_k^h} a_{mn}^2 = 1 + \sum_{j=1}^{J} \sum_{n_j \in S_j} a_{m,n_j}^2 \lesssim 1 + \sum_{j=1}^{J} j^{-2\alpha+1} k^{-2\alpha\delta}$$

$$\lesssim \begin{cases} 1 + k^{2(1-\delta-\alpha)} \lesssim k^{2(1-\delta-\alpha)}, & \alpha < 1,\ \alpha < 1-\delta < 1 \\ 1 + k^{-2\delta} \ln k \lesssim 1, & \alpha = 1,\ 0 < \delta < 1 \\ 1 + k^{-2\alpha\delta} \lesssim 1, & \alpha > 1,\ 0 < \delta < 1 \end{cases} \tag{60}$$

As a matter of fact, for any grid point $\mathbf{y}_m$, each j-th square neighbors of $\mathbf{y}_m$ has at least $8j/4 = 2j$ points for $j = 1, 2, \ldots, J \sim k^{1-\delta}$, e.g., if $\mathbf{y}_m$ is a corner point of the unit square. Hence the above asymptotic formula is still true. For a fixed $\alpha > 0$ and any $0 < \delta < 1$ arbitrary close to 0, we have

$$\sum_{m=1}^{n_k^\epsilon} \lambda_m^2 \le \sum_{m=1}^{n_k^h} \sum_{n=1}^{n_k^h} a_{mn}^2 \lesssim \begin{cases} k^{2(2(1-\delta)-\alpha)}, & \alpha < 1 \\ k^{2(1-\delta)}, & \alpha \ge 1 \end{cases} \tag{61}$$

Combining (61) with (54), one gets

$$\underline{N}_k^\epsilon \gtrsim \begin{cases} (1-\epsilon^2)^2 k^{2\alpha}, & \alpha < 1 \\ (1-\epsilon^2)^2 k^{2(1-\delta)}, & \alpha \ge 1. \end{cases} \tag{62}$$

Combining (61) with (55), one gets

$$\overline{N}_k^\epsilon \lesssim \begin{cases} \epsilon^{-4} k^{2(2(1-\delta)-\alpha)}, & \alpha < 1 \\ \epsilon^{-4} k^{2(1-\delta)}, & \alpha \ge 1 \end{cases} . \tag{63}$$

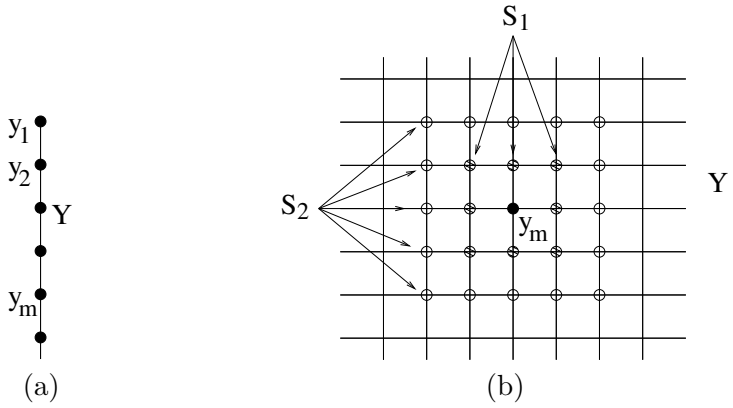

FIGURE 6. Green's functions with sources on a uniform grid.

Case 3: $s = 3$, Y is a unit cube in R^3. Let $\mathbf{y}_m, m = 1, 2, \ldots, n_k^h = k^{3(1-\delta)}$ be the grid points of a uniform grid in Y with a grid size $h = k^{\delta-1}, 0 < \delta < 1$ and define matrix A as in (52). Let $\lambda_1 \geq \lambda_2 \geq \ldots \geq \lambda_{n_k^h} \geq 0$ be its eigenvalues, then $\sum_{m=1}^{n_k^h} \lambda_m = n_k^h$ and we have (54), (55). Similar to 2D case, assume $\mathbf{y}_m$ is the center of the cube. We divide all other points into groups of 1st cube neighbors, 2nd cube neighbors, ..., j-th cube neighbors, denoted by $C_j, j = 1, 2, \ldots, J \sim h^{-1} = k^{1-\delta}$. C_j contains those $6(2j+1)^2 - 12(2j+1) + 8 = 24j^2 + 2$ grid points $\mathbf{y}_{n_j}$ that are on the faces of the j-th cube centered at $\mathbf{y}_m$ with each face a square whose side is of length $2jh$. We have $jh \leq |\mathbf{y}_{n_j} - \mathbf{y}_m| \leq \sqrt{3}jh, \mathbf{y}_{n_j} \in C_j$, and $a_{m,n_j} \lesssim (kjh)^{-\alpha} = j^{-\alpha}k^{-\alpha\delta}$. For $0 < \delta < 1$ arbitrary close to 0, one has the row sum estimate

$$\sum_{n=1}^{n_k^h} a_{mn}^2 = 1 + \sum_{j=1}^{J} \sum_{n_j \in C_j} a_{m,n_j}^2 \lesssim 1 + \sum_{j=1}^{J} (24j^2 + 2) j^{-2\alpha} k^{-2\alpha\delta}$$

$$\lesssim \begin{cases} 1 + k^{3(1-\delta)-2\alpha} \lesssim k^{3(1-\delta)-2\alpha}, & \alpha < \frac{3}{2},\ \frac{2}{3}\alpha < 1 - \delta < 1 \\ 1 + k^{-3\delta} \ln k \lesssim 1, & \alpha = \frac{3}{2},\ 0 < \delta < 1 \\ 1 + k^{-2\alpha\delta} \lesssim 1, & \alpha > \frac{3}{2},\ 0 < \delta < 1. \end{cases} \tag{64}$$

Also this is true for any point $\mathbf{y}_m$ which has at least $1/8$ of $24j^2 + 2$ points in its j-th cube neighbors C_j for $j = 1, 2, \ldots, J \sim k^{1-\delta}$, e.g., if $\mathbf{y}_m$ is a corner point of the unit cube. Hence for a fixed $\alpha > 0$ and any $0 < \delta < 1$ arbitrary close to 0,

$$\sum_{m=1}^{n_k^\epsilon} \lambda_m^2 \leq \sum_{m=1}^{n_k^h} \sum_{n=1}^{n_k^h} a_{mn}^2 \lesssim \begin{cases} k^{2(3(1-\delta)-\alpha)}, & \alpha < \frac{3}{2} \\ k^{3(1-\delta)}, & \alpha \geq \frac{3}{2} \end{cases} \tag{65}$$

Combining (65) with (54), one gets

$$\underline{N}_k^\epsilon \gtrsim \begin{cases} (1-\epsilon^2)^2 k^{2\alpha}, & \alpha < \frac{3}{2} \\ (1-\epsilon^2)^2 k^{3(1-\delta)}, & \alpha \geq \frac{3}{2} \end{cases}. \tag{66}$$

Combine (65) with (55), one gets

$$\overline{N}_k^\epsilon \lesssim \begin{cases} \epsilon^{-4} k^{2(3(1-\delta)-\alpha)}, & \alpha < \frac{3}{2} \\ \epsilon^{-4} k^{3(1-\delta)}, & \alpha \geq \frac{3}{2} \end{cases}. \tag{67}$$

Replace $s\delta$ by δ in each of the above cases, we complete the proof.

In the above estimates for all cases, the constant in $\lesssim$ involves the constant in the correlation of two Green's functions (49), which depends on X, Y and the distance in-between (see estimates in the previous section), and universal constants in the estimate of the row sum of matrix A. □

Remark 3.1. *When $d = 3$, if either $\dim(X) = \dim(Y) = 3$ or X and Y are separated, there are $0 < \underline{c} < \overline{c} < \infty$ independent of k such that $\underline{c} \leq \|G_0(\cdot, \mathbf{y})\|_2 \leq \overline{c}, \forall \mathbf{y} \in$*

Y. For the same set of Green's functions $G_0(\mathbf{x}, \mathbf{y}_j)$ as in the above proof and $A =< G_0(\cdot, \mathbf{y}_m), G_0(\cdot, \mathbf{y}_n) >$, we have

$$\underline{c}^2 n_k^h \le \sum_{m=1}^{n_k^h} \lambda_m \le \overline{c}^2 n_k^h \quad \Rightarrow \sum_{m=1}^{\underline{N}_k^\epsilon} \lambda_m \ge (1-\epsilon^2) \sum_{m=1}^{n_k^h} \lambda_m \ge (1-\epsilon^2)\underline{c}^2 n_k^h. \tag{68}$$

Hence inequalities (54) *is replaced by the following:*

$$\sum_{m=1}^{n_k^h} \lambda_m^2 > \sum_{m=1}^{\underline{N}_k^\epsilon} \lambda_m^2 \ge \underline{N}_k^\epsilon \left[\frac{(1-\epsilon^2)\underline{c}^2 n_k^h}{\underline{N}_k^\epsilon} \right]^2 = \frac{[(1-\epsilon^2)\underline{c}^2 n_k^h]^2}{\underline{N}_k^\epsilon}, \tag{69}$$

and (55) *is the same. The previous estimates of $\sum_{m=1}^{n_k^\epsilon} \lambda_m^2 \le \sum_{m=1}^{n_k^h} \sum_{n=1}^{n_k^h} a_{mn}^2$ is amplified by $\overline{c}^4$ at most. So the same results are true by adding a factor of $\underline{c}^4 \overline{c}^{-4}$.*

When $d = 2$, except for a scaling factor $k^{-\frac{1}{2}}$ for the Green's function, everything else is similar to the case $d = 3$. By the Definition 3.2, $\underline{N}_k^\epsilon$ is independent of a constant scaling of the whole set of vectors. So the results for $\underline{N}_k^\epsilon$ also holds for $A =< G_0(\cdot, \mathbf{y}_m), G_0(\cdot, \mathbf{y}_n) >$.

Remark 3.2. *The size of Y can be scaled into the result of Lemma 3.1, e.g., if Y is scaled to aY then k is scaled to ak. If $\alpha \ge \frac{s}{2}$, trace estimates* (56), (61), *and* (65) *gives $\sum_{m=1}^{n_k^h} \lambda_m^2 \lesssim n_k^h$. It can be seen easily from* (54) *and* (55) *that if Y is scaled to aY, it is equivalent to scaling k to ak in n_k^h and in those estimates* (50), (51) *for $\underline{N}_k^\epsilon$ and $\overline{N}_k^\epsilon$ respectively. The only factor that can not be scaled with n_k^h in the trace estimates is $k^{-2\alpha\delta}$ in* (56), (60) *and* (64). *Hence, in addition to scaling k to ak, there is an extra factor of $a^{2\alpha\delta}$ for the result of Lemma 3.1. However, this factor goes to 1 as $\delta \to 0$ for a fixed $a > 0$.*

Remark 3.3. *The key estimates in the proof of Lemma 3.1 are* (54) *(or* (69)*),* (55), *and the one for $\sum_{m=1}^{n_k^h} \lambda_m^2 = tr(A^T A)$. Although the estimate of $tr(A^T A)$ can be improved by a more careful estimate of each row sum $\sum_{n=1}^{n_k^h} a_{mn}^2$ by taking into account different decorrelation rate according to Theorem 2.1. For example, by dividing those points in each j-th square (cube) neighbors of $\mathbf{y}_m$ (see Figure 6) into directional cone sections according to whether the line connecting $\mathbf{y}_m$ and its neighbors intersecting X or not, one gets different decorrelation rates of two Green's functions, i.e., different power α in $a_{m,n_j} \lesssim (kjh)^{-\alpha}$ for points in different cones. However, as long as there is a solid angle cone such that lines connecting those neighbors in that cone and $\mathbf{y}_m$ intersect X, the order of the estimate can not be improved. On the other hand, whether* (54) *and* (55) *are sharp or not is an interesting but difficult question. The answer depends on the variation of leading eigenvalues of the matrix $A =< \hat{G}_0(\cdot, \mathbf{y}_m), \hat{G}_0(\cdot, \mathbf{y}_n) >$, which depends on the geometric setup of X and Y, and ϵ.*

3.2. **Lower bound and upper bound estimates for the approximate separability of the Green's functions of the Helmholtz equation in the high frequency limit.** We first use Lemma 3.1 to prove the following lower bound estimate for the approximate separability (12) of the Green's functions of the Helmholtz equation (3) in the high frequency limit.

Theorem 3.1. *Let X, Y be two compact manifolds embedded in $R^d, d = 2, 3$, and $d \geq \dim(X) \geq \dim(Y) = s$. If there is a $\alpha > 0$ such that for any two points $\mathbf{y}_1, \mathbf{y}_2 \in Y$,*

$$| < \hat{G}_0(\cdot, \mathbf{y}_1), \hat{G}_0(\cdot, \mathbf{y}_2) >_X | \lesssim (k|\mathbf{y}_1 - \mathbf{y}_2|)^{-\alpha} \quad \text{as } k|\mathbf{y}_1 - \mathbf{y}_2| \to \infty$$

and there are $f_l(\mathbf{x}) \in L_2(X), g_l(\mathbf{y}) \in L_2(Y), l = 1, 2, \ldots, N_k^\epsilon$ such that

$$\left\| \hat{G}_0(\mathbf{x}, \mathbf{y}) - \sum_{l=1}^{N_k^\epsilon} f_l(\mathbf{x}) g_l(\mathbf{y}) \right\|_{L_2(X \times Y)} \leq \epsilon, \tag{70}$$

then

$$N_k^\epsilon \geq \begin{cases} c_\epsilon k^{2\alpha}, & \alpha < \frac{s}{2}, \\ c_\epsilon k^{s-\delta}, & \alpha \geq \frac{s}{2}, \end{cases} \tag{71}$$

for any $\delta > 0$ and k large enough, where $c_\epsilon \geq c(1 - (C\epsilon)^2)^2$ for some positive constants c and C that depend on X, Y and the distance in-between.

Proof. Without loss of generality, we assume that Y is a unit interval, a unit square or a unit cube for $s = 1, 2, 3$ respectively. First, divide Y into uniform cells, $Y_m, m = 1, 2, \ldots N_k^{\overline{h}} = k^{s(1-\delta)}$, with a cell size $\overline{h} = k^{\delta - 1}$, for any $\delta > 0$ arbitrary close to 0. Then divide each cell $Y_m^{\overline{h}}$ further into uniform finer cells of size $\underline{h} < k^{-1}$, $Y_{m,n}^{\underline{h}}, n = 1, 2, \ldots, N_{\underline{k}}^{\underline{h}} = (\overline{h}/\underline{h})^s$. See Figure 7. $\underline{h}$ needs to be small enough, which will be determined later. For a fixed n, $Y_{m,n}^{\underline{h}}$ is in the same relative location in each coarse cell $Y_m^{\overline{h}}$. The center and volume of each cell $Y_{m,n}^{\underline{h}}$ is $\mathbf{y}_{m,n}$ and $\underline{h}^s$ respectively. Define $\hat{G}_0^{\underline{h}}(\mathbf{x}, \mathbf{y}) = \hat{G}_0(\mathbf{x}, \mathbf{y}_{m,n}), \mathbf{y} \in Y_{m,n}^{\underline{h}}$ to be a piecewise constant function in $\mathbf{y}$.

If X, Y are disjoint, we have $|\nabla_{\mathbf{y}} \hat{G}_0(\mathbf{x}, \mathbf{y})| \lesssim k$ uniformly in $\mathbf{x} \in X$ and $\mathbf{y} \in Y$. For any $\epsilon > 0$, one can pick $\underline{h} < k^{-1}$ small enough such that

$$|\hat{G}_0(\mathbf{x}, \mathbf{y}) - \hat{G}_0(\mathbf{x}, \mathbf{y}_{m,n})| \leq \epsilon, \quad \forall \mathbf{x} \in X, \mathbf{y} \in Y_{m,n}^{\underline{h}}, \quad m = 1, 2, \ldots, N_k^{\overline{h}}, n = 1, 2, \ldots, N_k^{\underline{h}}.$$

Hence

$$\int_Y d\mathbf{y} \int_X |\hat{G}_0(\mathbf{x}, \mathbf{y}) - \hat{G}_0^{\underline{h}}(\mathbf{x}, \mathbf{y})|^2 d\mathbf{x} = \sum_{m=1}^{N_k^{\overline{h}}} \sum_{n=1}^{N_k^{\underline{h}}} \int_{Y_{m,n}^{\underline{h}}} d\mathbf{y} \int_X |\hat{G}_0(\mathbf{x}, \mathbf{y}) - \hat{G}_0(\mathbf{x}, \mathbf{y}_{m,n})|^2 d\mathbf{x} \lesssim \epsilon^2 \tag{72}$$

If X, Y are not disjoint and $\mathbf{y} \in X \cap Y$, since $G_0(\cdot, \mathbf{y}) \in L_2(X)$ for $d = 2, 3$, we show that there is still $\underline{h} < k^{-1}$ small enough such that

$$\int_X |\hat{G}_0(\mathbf{x}, \mathbf{y}) - \hat{G}_0(\mathbf{x}, \mathbf{y}_{m,n})|^2 d\mathbf{x} \lesssim \epsilon^2, \quad \text{if } \mathbf{y} \in Y_{m,n}^{\underline{h}}, \tag{73}$$

which implies (72). From (10) and the asymptotic formulas (5), (6), we have

$$\int_{B_\tau(\mathbf{y})} |\hat{G}_0(\mathbf{x}, \mathbf{y})|^2 d\mathbf{x} \lesssim \tau \tag{74}$$

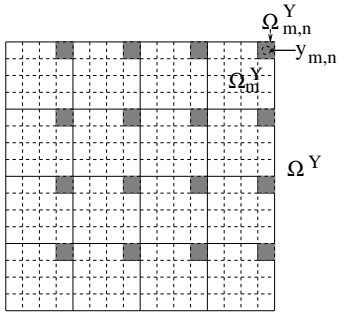

FIGURE 7. Two scale decomposition of the source domain.

with the constant independent of k, where $B_\tau(\mathbf{y})$ denotes the ball with radius τ centered at $\mathbf{y}$. Hence there are balls $B_{\tau(\epsilon)}(\mathbf{y})$ and $B_{\tau(\epsilon)}(\mathbf{y}_{m,n})$ with radius $\tau(\epsilon) \sim \epsilon^2$ such that

$$\int_{X\cap B_{\tau(\epsilon)}(\mathbf{y})} |\hat{G}_0(\mathbf{x},\mathbf{y})|^2 d\mathbf{x} \le \epsilon^2, \quad \int_{X\cap B_{\tau(\epsilon)}(\mathbf{y}_{m,n})} |\hat{G}_0(\mathbf{x},\mathbf{y}_{m,n})|^2 d\mathbf{x} \le \epsilon^2 \tag{75}$$

for a given $\epsilon > 0$. Denote $X_\epsilon = X \cap (B_{\tau(\epsilon)}(\mathbf{y}) \cup B_{\tau(\epsilon)}(\mathbf{y}_{m,n}))$ and $X_\epsilon^C = X \setminus X_\epsilon$. For $\mathbf{y} \in Y^h_{m,n}$ we have

$$\begin{aligned}
&\textstyle\int_X |\hat{G}_0(\mathbf{x},\mathbf{y}) - \hat{G}_0(\mathbf{x},\mathbf{y}_{m,n})|^2 d\mathbf{x} \\
&= \textstyle\int_{X_\epsilon^C} |\hat{G}_0(\mathbf{x},\mathbf{y}) - \hat{G}_0(\mathbf{x},\mathbf{y}_{m,n})|^2 d\mathbf{x} + \int_{X_\epsilon} |\hat{G}_0(\mathbf{x},\mathbf{y}) - \hat{G}_0(\mathbf{x},\mathbf{y}_{m,n})|^2 d\mathbf{x} = I + II
\end{aligned}$$

Since $|\nabla_{\mathbf{y}} \hat{G}_0(\mathbf{x},\mathbf{y})| \lesssim \max(k\tau^{-1}(\epsilon), \tau^{-2}(\epsilon))$, $\forall \mathbf{x} \in X_\epsilon^C$, by choosing $\underline{h} < k^{-1}$ small enough we get $I \lesssim \epsilon^2$. From (75) we get $II \lesssim \epsilon^2$. Hence we prove (73).

Define the linear subspace $S_X = \text{span}\{f_l(\mathbf{x})\}_{l=1}^{N_k^\epsilon} \subset L_2(X)$, then

$$\int_Y \|\hat{G}_0(\mathbf{x},\mathbf{y}) - P_{S_X}\hat{G}_0(\mathbf{x},\mathbf{y})\|^2_{L_2(X)} d\mathbf{y} \le \epsilon^2,$$

where P_{S_X} denotes the projection to S_X in $L_2(X)$. From (72), we have

$$\int_Y \|(I - P_{S_X})[\hat{G}_0(\mathbf{x},\mathbf{y}) - \hat{G}_0^{\underline{h}}(\mathbf{x},\mathbf{y})]\|^2_{L_2(X)} d\mathbf{y} \lesssim \epsilon^2,$$

where I is the identity map. From the above two inequalities we have

$$\begin{aligned}
\epsilon^2 &\gtrsim \textstyle\int_Y \|(I-P_{S_X})\hat{G}_0^{\underline{h}}(\mathbf{x},\mathbf{y})]\|^2_{L_2(X)}d\mathbf{y} \\
&= \textstyle\sum_{m=1}^{N_k^{\overline{h}}}\sum_{n=1}^{N_k^{\underline{h}}}\int_{Y_{m,n}^{\underline{h}}}\|(I-P_{S_X})\hat{G}_0(\mathbf{x},\mathbf{y}_{m,n})\|^2_{L_2(X)}d\mathbf{y} \\
&= \underline{h}^s\textstyle\sum_{m=1}^{N_k^{\overline{h}}}\sum_{n=1}^{N_k^{\underline{h}}}\|\hat{G}_0(\mathbf{x},\mathbf{y}_{m,n})-P_{S_X}\hat{G}_0(\mathbf{x},\mathbf{y}_{m,n})\|^2_{L_2(X)} \qquad (76)\\
&= (\underline{h}/\overline{h})^s\overline{h}^s\textstyle\sum_{m=1}^{N_k^{\overline{h}}}\sum_{n=1}^{N_k^{\underline{h}}}\|\hat{G}_0(\mathbf{x},\mathbf{y}_{m,n})-P_{S_X}\hat{G}_0(\mathbf{x},\mathbf{y}_{m,n})\|^2_{L_2(X)} \\
&\gtrsim \tfrac{1}{N_k^{\underline{h}}}\textstyle\sum_{n=1}^{N_k^{\underline{h}}}\tfrac{1}{N_k^{\overline{h}}}\sum_{m=1}^{N_k^{\overline{h}}}\|\hat{G}_0(\mathbf{x},\mathbf{y}_{m,n})-P_{S_X}\hat{G}_0(\mathbf{x},\mathbf{y}_{m,n})\|^2_{L_2(X)}
\end{aligned}$$

Assume

$$\begin{aligned}
&\sum_{m=1}^{N_k^{\overline{h}}}\|\hat{G}_0(\mathbf{x},\mathbf{y}_{m,\overline{n}})-P_{S_X}\hat{G}_0(\mathbf{x},\mathbf{y}_{m,\overline{n}})\|^2_{L_2(X)} \\
=&\min_n\sum_{m=1}^{N_k^{\overline{h}}}\|\hat{G}_0(\mathbf{x},\mathbf{y}_{m,n})-P_{S_X}\hat{G}_0(\mathbf{x},\mathbf{y}_{m,n})\|^2_{L_2(X)},
\end{aligned} \qquad (77)$$

then there is a constant $C>0$ such that

$$\frac{1}{N_k^{\overline{h}}}\sum_{m=1}^{N_k^{\overline{h}}}\|\hat{G}_0(\mathbf{x},\mathbf{y}_{m,\overline{n}})-P_{S_X}\hat{G}_0(\mathbf{x},\mathbf{y}_{m,\overline{n}})\|^2_{L_2(X)}\le C^2\epsilon^2. \qquad (78)$$

Since $\mathbf{y}_{m,\overline{n}}\in Y, m=1,2,\dots N_k^{\overline{h}}=k^{s(1-\delta)}$ forms a uniform grid with the grid size $\overline{h}=k^{\delta-1}$, we apply Lemma 3.1 to get

$$\dim(S_X)\ge\begin{cases} c(1-(C\epsilon)^2)^2k^{2\alpha} & \alpha<\frac{s}{2} \\ c(1-(C\epsilon)^2)^2k^{s-\delta} & \alpha\ge\frac{s}{2}\end{cases}$$

for any $\delta>0$ and arbitrary close to 0 as $k\to\infty$, where $C>0, c>0$ are some constants that depend only on X,Y and the distance in-between.

□

Remark 3.4. *In three dimensions, the same lower bound estimates for the approximate separability hold for the unnormalized Green's functions of the Helmholtz equation in the high frequency limit as well. Theorem 3.1 reveals the intrinsic complexity for numerical computations of the Helmholtz equation with a large wave number k in three dimensions. In other words, the degrees of freedom have to grow with certain powers of k no matter what bases are used to approximate general solutions to the PDE due to the rapid decorrelation of the Green's functions. The result also implies that low rank approximations do not exist*

for off-diagonal submatrices of the inverse matrix of the linear system corresponding to a discretization with mesh size h that satisfies $hk \sim$constant. However, in two dimensions, for separated X and Y, $|G_0(\mathbf{x},\mathbf{y})| \lesssim k^{-\frac{1}{2}}, \forall(\mathbf{x},\mathbf{y}) \in X \times Y$ as $k \to \infty$ due to the energy localization near the source as shown in (9). Hence, approximate separability for unnormalized Green's functions of the Helmholtz equation in two dimensions for separated X, Y is trivial in the high frequency limit. This mitigates the difficulty in numerical computations of the Helmholtz equation to some extent for large k in 2D.

Next we give an upper bound estimate for the approximate separability of the Green's functions of the Helmholtz equation in the high frequency limit. The intuition is that two Green's functions with sources located within a wavelength are correlated. So the linear subspace spanned by the Green's functions sampled in the source domain with a separation distance smaller than a wavelength should approximate the whole family of Green's functions good enough.

Theorem 3.2. *Let X, Y be two compact manifolds embedded in $R^d, d = 2, 3$ and $d \geq \dim(X) \geq \dim(Y) = s$. For any $\epsilon > 0$ and $\delta > 0$, there are $f_l(\mathbf{x}) \in L_2(X), g_l(\mathbf{y}) \in L_2(Y), l = 1, 2, \ldots, N_k^\epsilon \lesssim k^{s+\delta}$ such that*

$$\left\| \hat{G}_0(\mathbf{x},\mathbf{y}) - \sum_{l=1}^{N_k^\epsilon} f_l(\mathbf{x}) g_l(\mathbf{y}) \right\|_{L_2(X\times Y)} \leq \epsilon \tag{79}$$

for k large enough, where the constant in $\lesssim$ depends on X, Y and the distance in-between.

Proof. Without loss of generality, assume Y is a unit interval, a unit square or a unit cube for $s = 1, 2, 3$ respectively. Let $\mathbf{y}_m, m = 1, 2, \ldots, N_k^h = k^{s(1+\delta/2)}$ be the grid points of a uniform grid in Y with a grid size $h = k^{-1-\delta/2}$. Denote the liner subspace $S_X = \text{span}\{\hat{G}_0(\mathbf{x},\mathbf{y}_m)\}_{m=1}^{N_k^h} \subset L_2(X)$. We show that

$$\|\hat{G}_0(\mathbf{x},\mathbf{y}) - P_{S_X}\hat{G}_0(\mathbf{x},\mathbf{y})\|_{L_2(X)} \leq \epsilon \tag{80}$$

for k large enough, where P_{S_X} denotes the projection to S_X in $L_2(X)$.

If X and Y are disjoint, we have $|\nabla_{\mathbf{y}}\hat{G}_0(\mathbf{x},\mathbf{y})| \lesssim k, \|D^2_{\mathbf{y}}\hat{G}_0(\mathbf{x},\mathbf{y})\| \lesssim k^2$, where the bound is uniform in $\mathbf{x}, \mathbf{y}$ and the constants in $\lesssim$ depend on the distance between X and Y. Given a non-grid point $\mathbf{y} \in Y$, $\hat{G}_0(\mathbf{x},\mathbf{y})$ can be approximated by a linear interpolation, which is a convex combination of the Green's functions at its neighboring grid points. To be precise, suppose $\mathbf{y} \in Y$ lies in the s dimensional simplex with vertices $\mathbf{y}_{m_1}, \ldots, \mathbf{y}_{m_{s+1}}$. Let $r^1_{\mathbf{y}}, \ldots, r^{s+1}_{\mathbf{y}}$ be the barycentric coordinates for $\mathbf{y}$, i.e.,

$$\mathbf{y} = \sum_{j=1}^{s+1} r^j_{\mathbf{y}} \mathbf{y}_{m_j}, \quad 1 \geq r^j_{\mathbf{y}} \geq 0, \quad \sum_{j=1}^{s+1} r^j_{\mathbf{y}} = 1.$$

Then we have the following linear interpolation

$$|\hat{G}_0(\mathbf{x},\mathbf{y}) - \sum_{j=1}^{s+1} r^j_{\mathbf{y}} \hat{G}_0(\mathbf{x},\mathbf{y}_{m_j})| \lesssim \|D^2_{\mathbf{y}}\hat{G}_0(\mathbf{x},\mathbf{y})\| h^2 \lesssim k^{-\delta}, \tag{81}$$

and hence (80) is true when k is large enough.

If X and Y are not disjoint and $\mathbf{y} \in X \cap Y$, one has $\hat{G}_0(\cdot, \mathbf{y}) \in L_2(X)$ for $d = 2, 3$. For a given $\epsilon > 0$, there are balls $B_{\tau(\epsilon)}(\mathbf{y})$ and $B_{\tau(\epsilon)}(\mathbf{y}_{m_j})$ with radius $0 < \tau(\epsilon) \sim \epsilon^2$ centered at $\mathbf{y}$ and $\mathbf{y}_{m_j}, j = 1, 2, \ldots, d+1$ such that

$$\int_{B_{\tau(\epsilon)}(\mathbf{y})} |\hat{G}_0(\mathbf{x}, \mathbf{y})|^2 d\mathbf{x} \leq \frac{\epsilon^2}{8(d+2)}, \quad \int_{B_{\tau(\epsilon)}(\mathbf{y}_{m_j})} |\hat{G}_0(\mathbf{x}, \mathbf{y}_{m_j})|^2 d\mathbf{x} \leq \frac{\epsilon^2}{8(d+2)}. \tag{82}$$

For any $\mathbf{x} \in X \setminus B_{\tau(\epsilon)}(\mathbf{y}) \cup (\cup_{j=1}^{d+1} B_{\tau(\epsilon)}(\mathbf{y}_{m_j}))$, we have

$$|\nabla_{\mathbf{y}} \hat{G}_0(\mathbf{x}, \mathbf{y})| \lesssim \max(k\tau^{-1}(\epsilon), \tau^{-2}(\epsilon)), \quad \|D^2_{\mathbf{y}} \hat{G}_0(\mathbf{x}, \mathbf{y})\| \lesssim \max(k^2\tau^{-1}(\epsilon), k\tau^{-2}(\epsilon), \tau^{-3}(\epsilon)),$$

and hence

$$\begin{aligned} |\hat{G}_0(\mathbf{x}, \mathbf{y}) - \sum_{j=1}^{s+1} r_{\mathbf{y}}^j \hat{G}_0(\mathbf{x}, \mathbf{y}_{m_j})| &\lesssim \|D^2_{\mathbf{y}} \hat{G}_0(\mathbf{x}, \mathbf{y})\| h^2 \\ &\lesssim \max(k^{-\delta}\tau^{-1}(\epsilon), k^{-1-\delta}\tau^{-2}(\epsilon), k^{-2-\delta}\tau^{-3}(\epsilon)). \end{aligned} \tag{83}$$

By decomposing the integration on X into two parts, one on $X_\epsilon = X \cap (B_{\tau(\epsilon)}(\mathbf{y}) \cup (\cup_{j=1}^{d+1} B_{\tau(\epsilon)}(\mathbf{y}_{m_j})))$ and the other on $X_\epsilon^C = X \setminus (B_{\tau(\epsilon)}(\mathbf{y}) \cup (\cup_{j=1}^{d+1} B_{\tau(\epsilon)}(\mathbf{y}_{m_j})))$, we have

$$\begin{aligned} &\textstyle\int_{X_\epsilon} |\hat{G}_0(\mathbf{x}, \mathbf{y}) - \sum_{j=1}^{d+1} r_{\mathbf{y}}^j \hat{G}_0(\mathbf{x}, \mathbf{y}_{m_j})|^2 d\mathbf{x} \\ &\leq 2 \textstyle\int_{X_\epsilon} |\hat{G}_0(\mathbf{x}, \mathbf{y})|^2 + \sum_{j=1}^{d+1} r_{\mathbf{y}}^j |\hat{G}_0(\mathbf{x}, \mathbf{y}_{m_j})|^2 d\mathbf{x} \\ &\leq 2 \textstyle\int_{B_{\tau(\epsilon)}(\mathbf{y}) \cup (\cup_{j=1}^{d+1} B_{\tau(\epsilon)}(\mathbf{y}_{m_j}))} |\hat{G}_0(\mathbf{x}, \mathbf{y})|^2 + \sum_{j=1}^{d+1} r_{\mathbf{y}}^j |\hat{G}_0(\mathbf{x}, \mathbf{y}_{m_j})|^2 d\mathbf{x} \\ &\leq \frac{\epsilon^2}{2}, \end{aligned} \tag{84}$$

and from (83)

$$\int_{X_\epsilon^C} |\hat{G}_0(\mathbf{x}, \mathbf{y}) - \sum_{j=1}^{d+1} r_{\mathbf{y}}^j \hat{G}_0(\mathbf{x}, \mathbf{y}_{m_j})|^2 d\mathbf{x} \leq \frac{\epsilon^2}{2} \tag{85}$$

when k is large enough. Combining the above two parts we get (80) when k is large enough, which implies

$$\sqrt{\int_Y \|\hat{G}_0(\mathbf{x}, \mathbf{y}) - P_{S_X} \hat{G}_0(\mathbf{x}, \mathbf{y})\|^2_{L_2(X)} d\mathbf{y}} \leq \epsilon. \tag{86}$$

□

Remark 3.5. *The above upper bound holds for unnormalized Green's function when $d = 3$.*

If $\dim(X) = \dim(Y) = d = 2, 3$, since the Green's function belongs to $L_2(X \times Y)$, our approximate separability estimates in L_2 norm is valid for general compact domains X and Y, disjoint or not. However, if X and Y are disjoint, our results in L_2 norm can be easily extended to $L_\infty(X \times Y)$. Since L_∞ norm is stronger than L_2 norm in a compact domain the lower bound estimates in Theorem 3.1 immediately extend to L_∞ norm. Also, the first part of the proof in Theorem 3.2 directly extends to L_∞ norm and hence the upper bound estimates. We summarize these two results below.

Theorem 3.3. *Let X, Y be two disjoint compact manifolds embedded in $R^d, d = 2, 3$, and $d \geq \dim(X) \geq \dim(Y) = s$. If there is a $\alpha > 0$ such that for any two points $\mathbf{y}_1, \mathbf{y}_2 \in Y$,*

$$| < \hat{G}_0(\cdot, \mathbf{y}_1), \hat{G}_0(\cdot, \mathbf{y}_2) >_X | \lesssim (k|\mathbf{y}_1 - \mathbf{y}_2|)^{-\alpha} \quad \text{as } k|\mathbf{y}_1 - \mathbf{y}_2| \to \infty$$

and there are $f_l(\mathbf{x}) \in L_\infty(X), g_l(\mathbf{y}) \in L_\infty(Y), l = 1, 2, \ldots, N_k^\epsilon$ such that

$$\left| \hat{G}_0(\mathbf{x}, \mathbf{y}) - \sum_{l=1}^{N_k^\epsilon} f_l(\mathbf{x}) g_l(\mathbf{y}) \right| \leq \epsilon, \quad \forall \mathbf{x} \in X, \forall \mathbf{y} \in Y, \tag{87}$$

then

$$N_k^\epsilon \geq \begin{cases} c_\epsilon k^{2\alpha}, & \alpha < \frac{s}{2}, \\ c_\epsilon k^{d-\delta}, & \alpha \geq \frac{s}{2}, \end{cases} \tag{88}$$

for any $\delta > 0$ and k large enough, where $c_\epsilon \geq c(1 - (C\epsilon)^2)^2$ for some positive constants c and C that depend on X, Y and the distance in-between.

Theorem 3.4. *Let X, Y be two disjoint compact manifolds embedded in $R^d, d = 2, 3$, and $d \geq \dim(X) \geq \dim(Y) = s$. For any $\epsilon > 0$ and $\delta > 0$, there are $f_l(\mathbf{x}) \in L_\infty(X), g_l(\mathbf{y}) \in L_\infty(Y), l = 1, 2, \ldots, N_k^\epsilon \leq Ck^{d+\delta}$ such that*

$$\left| \hat{G}_0(\mathbf{x}, \mathbf{y}) - \sum_{l=1}^{N_k^\epsilon} f_l(\mathbf{x}) g_l(\mathbf{y}) \right| \leq \epsilon, \quad \forall \mathbf{x} \in X, \forall \mathbf{y} \in Y, \tag{89}$$

for k large enough, where $C > 0$ is some constant that depends on X, Y and the distance in-between.

Remark 3.6. *In Theorem 3.2, the upper bound estimate for the approximate separability of the Green's functions of the Helmholtz equation in the high frequency limit in L_2 norm is derived based on a separable approximation using linear combinations (interpolation) of a set of Green's functions with sources properly sampled. In practice, a set of properly sampled Green's functions can also be viewed as a set of learned basis to represent general solutions to the underlying PDE effectively. One can also construct separable approximations for the Green's functions using the eigenfunctions of the differential operator, which can be viewed as the spectrum basis for the representation of general solutions to the underlying PDE. Below we show that, based on a separable approximation using the eigenfunctions of the Laplace operator and Weyl's asymptotic formula* [30] *for the eigenvalues, we can*

obtain exactly the same upper bound estimate in the L_2 norm as in Theorem 3.2 for the approximate separability of the Green's functions of the Helmholtz equation in the high frequency limit in a bounded domain.

Suppose $G(\mathbf{x},\mathbf{y})$ is the Green's function in a bounded domain $\Omega \subset R^d$ satisfying

$$\begin{cases} \Delta_{\mathbf{x}} G(\mathbf{x},\mathbf{y}) + k^2 G(\mathbf{x},\mathbf{y}) = \delta(\mathbf{x}-\mathbf{y}), & \mathbf{x},\mathbf{y} \in \Omega, \\ G(\mathbf{x},\mathbf{y}) = 0, & \mathbf{x} \in \partial\Omega. \end{cases} \tag{90}$$

Let $u_m(\mathbf{x}), \|u_m\|_{L_2(\Omega)} = 1, m = 1, 2, \ldots$ be the normalized eigenfunctions for the Laplace operator

$$\begin{cases} \Delta u_m(\mathbf{x}) = \lambda u_m(\mathbf{x}), & \mathbf{x} \in \Omega, \\ u_m(\mathbf{x}) = 0, & \mathbf{x} \in \partial\Omega \end{cases} \tag{91}$$

with eigenvalues $0 > \lambda_1 \geq \lambda_2 \geq \ldots$. Hence $u_m(\mathbf{x}), m = 1, 2, \ldots$ are also the normalized eigenfunctions for the homogeneous Helmholtz operator with eigenvalues $\lambda_m + k^2, m = 1, 2, \ldots$. Here we assume the domain Ω is not resonant, i.e., $\lambda_m + k^2 \neq 0, \forall m$. Since $u_m(\mathbf{x})$ forms an orthonormal basis for $L_2(\Omega)$ and $G(\mathbf{x},\mathbf{y}) \in L_2(\Omega)$ for $d = 2, 3$, one has the following expansion

$$G(\mathbf{x},\mathbf{y}) = \sum_{m=1}^{\infty} (\lambda_m + k^2)^{-1} u_m(\mathbf{y}) u_m(\mathbf{x}). \tag{92}$$

The Weyl's asymptotic formula gives

$$|\lambda_m| \sim \frac{4\pi^2 m^{2/d}}{(C_d |\Omega|)^{2/d}} \tag{93}$$

for large m, where $|\Omega|$ is the volume of Ω. Choose a large enough integer $M \gtrsim k^{d+\delta}, \delta > 0$, then for $m > M$, $|\lambda_m + k^2|^{-1} \lesssim |\lambda_m|^{-1} \lesssim m^{-\frac{2}{d}}$. For any $\epsilon > 0$, we have

$$\int_\Omega \int_\Omega |G(\mathbf{x},\mathbf{y}) - \sum_{m=1}^{M} (\lambda_m + k^2)^{-1} u_m(\mathbf{y}) u_m(\mathbf{x})|^2 d\mathbf{x} d\mathbf{y} \lesssim \sum_{m=M+1}^{\infty} m^{-\frac{4}{d}} \lesssim M^{1-\frac{4}{d}} \leq \epsilon^2 \tag{94}$$

when k is large enough for $d = 2, 3$. In particular for any two subdomains X, Y of Ω, (94) implies

$$\begin{aligned} &\left\| G(\mathbf{x},\mathbf{y}) - \textstyle\sum_{m=1}^{M} (\lambda_m + k^2)^{-1} u_m(\mathbf{y}) u_m(\mathbf{x}) \right\|_{L_2(X\times Y)} \\ &\leq \left\| G(\mathbf{x},\mathbf{y}) - \textstyle\sum_{m=1}^{M} (\lambda_m + k^2)^{-1} u_m(\mathbf{y}) u_m(\mathbf{x}) \right\|_{L_2(\Omega\times\Omega)} \leq \epsilon \end{aligned} \tag{95}$$

which shows that $N_k^\epsilon \lesssim k^{d+\delta}$ for any $\delta > 0$ in the high frequency limit.

One can include the volume of Ω explicitly in the above argument by requiring $\frac{M}{|\Omega|} \gtrsim k^{d+\delta}$, which implies $N_k^\epsilon \lesssim |\Omega| k^{d+\delta}$. Instead of using Fourier series to show that the scattered field as a superposition of free space Green's functions is almost band limited and the degrees of freedom is close to the Nyquist number in term of the domain size in [5, 6], we generalize the result using the eigenfunctions of the Laplace operator.

Remark 3.7. *It can be seen from Theorem 3.1 and 3.2 as well as Remark 3.6 that if two Green's functions decorrelate fast,* $\left|< \hat{G}(\cdot, \mathbf{y}_1), \hat{G}(\cdot, \mathbf{y}_2) >\right| \lesssim (k|\mathbf{y}_1 - \mathbf{y}_2|)^{-\alpha}$ *with* $\alpha \geq \frac{s}{2}, s = \dim(Y) \leq \dim(X)$*, the upper and lower bound estimates of the approximate separability of the Green's functions of the Helmholtz equation in the high frequency limit is sharp. In this scenario, a set of Green's functions with sources properly sampled or a set of leading eigenfunctions for the Laplace operator form an effective basis to represent any Green's function or solution of the PDE. However, the representation is not further compressible.*

Remark 3.8. *Lemma 3.1 and Theorem 3.1 provide a necessary condition for high separability of the Green's functions: no fast decorrelation between two Green's functions. For example, the Green's functions of the following coercive elliptic operator in divergence form satisfy the necessary condition in* $R^d, d \geq 3$*,*

$$L = -\sum_{i,j=1}^{d} \frac{\partial}{\partial x_j}(a_{ij}(\mathbf{x})\frac{\partial}{\partial x_j}), \quad \lambda|\xi|^2 \leq \sum_{i,j=1}^{d} a_{ij}(\mathbf{x})\xi_i\xi_j \leq \mu|\xi|^2, \tag{96}$$

where $a_{ij}(\mathbf{x})$ *are bounded measurable functions and* $0 < \lambda \leq \mu < \infty$ *are two constants. The unique Green's function* $G(\mathbf{x}, \mathbf{y})$ *for the above differential operator in* $R^d, d \geq 3$ *satisfies* [22, 14]

$$c(d, \lambda, \mu)|\mathbf{x} - \mathbf{y}|^{2-d} \leq G(\mathbf{x}, \mathbf{y}) \leq C(d, \lambda, \mu)|\mathbf{x} - \mathbf{y}|^{2-d}, \tag{97}$$

where $0 < c(d, \lambda, \mu) < C(d, \lambda, \mu) < \infty$ *are two constants depending on* d, λ, μ*. Given a compact domain* $X \subset R^d$ *and two points* $\mathbf{y}_1, \mathbf{y}_2 \notin X$*, define*

$$\rho = \min[\min_{\mathbf{x}\in X} |\mathbf{x} - \mathbf{y}_1|, \min_{\mathbf{x}\in X} |\mathbf{x} - \mathbf{y}_2|], \quad K = \frac{C(d, \lambda, \mu)}{c(d, \lambda, \mu)} \left[1 + \frac{|\mathbf{y}_1 - \mathbf{y}_2|}{\rho}\right]^{d-2}.$$

Then we have

$$\frac{G(\mathbf{x}, \mathbf{y}_2)}{G(\mathbf{x}, \mathbf{y}_1)} \leq \frac{C(d, \lambda, \mu)}{c(d, \lambda, \mu)} \left[\frac{|\mathbf{x} - \mathbf{y}_1|}{|\mathbf{x} - \mathbf{y}_2|}\right]^{d-2} \leq \frac{C(d, \lambda, \mu)}{c(d, \lambda, \mu)} \left[\frac{|\mathbf{x} - \mathbf{y}_2| + |\mathbf{y}_1 - \mathbf{y}_2|}{|\mathbf{x} - \mathbf{y}_2|}\right]^{d-2} \leq K,$$

and vice versa. Given two disjoint compact domains $X, Y \subset R^d, d \geq 3$*, with* ρ *being the distance between the two domains and* r *being the diameter of* Y*, the correlation between two Green's functions with sources at* $\mathbf{y}_1, \mathbf{y}_2 \in Y$ *has the following property*

$$1 \geq < \hat{G}(\cdot, \mathbf{y}_1), \hat{G}(\cdot, \mathbf{y}_2) >_X \geq K^{-2} \geq \tilde{K}^{-2}, \quad \tilde{K} = \frac{C(d, \lambda, \mu)}{c(d, \lambda, \mu)} \left[1 + \frac{r}{\rho}\right]^{d-2}. \tag{98}$$

Furthermore, the Caccioppoli inequality gives a bound of the L_2 *norm of the gradient of the Green's function away from the source singularity. This fact was used in* [2] *to show that the Green's functions of the above elliptic operator is highly separable.*

4. Examples

In this section we study the approximate separability for the Green's function of the Helmholtz equation in the high frequency limit for concrete examples for disjoint X, Y in 3D in two scenarios:

(1) For two fixed compact manifolds X, Y embedded in R^3, we provide explicit lower and upper bound estimates in Section 4.1 based on our previous analysis.
(2) For special k dependent X, Y setups, we show the possibility of high separability in Section 4.2.

For the first scenario, the Green's functions of the Helmholtz equation are not highly separable in the high frequency limit since N_k^ϵ grows as some power of k. In particular, for two fixed compact manifolds X, Y embedded in R^3 and $3 \geq \dim(X) \geq \dim(Y) = s$, if the decorrelation of two Green's functions is fast enough,

$$\left| < \hat{G}(\cdot, \mathbf{y}_1), \hat{G}(\cdot, \mathbf{y}_2) >_X \right| \lesssim (k|\mathbf{y}_1 - \mathbf{y}_2|)^{-\alpha}, \quad \alpha \geq \frac{s}{2},$$

both the lower bound and the upper bound for the approximate separability of the Green's function of the Helmholtz equations in the high frequency limit are sharp. For example, as discussed in the proof of Theorem 2.1, Remark 2.3 and Section 2.2, if a ray going through two points, $\mathbf{y}_1, \mathbf{y}_2 \in Y$, does not intersect X or intersect X at isolated points, then $\alpha \geq \frac{s}{2}$ and hence both lower bound and upper bound are sharp.

However, if X and Y are allowed to be k dependent, there are special setups for which the Green's functions of the Helmholtz equation can be highly separable. High separability in these special setups, which implies the availability of low rank approximations in the corresponding discretized systems, can be utilized to develop fast algorithms.

In the following case studies, we give lower bound and upper bound estimates for N_k^ϵ with fixed $\epsilon > 0$ as $k \to \infty$. All constants in these estimates are independent of k. The dependence of the constants on X, Y as well as on ϵ (such as those in Theorem 3.1) are suppressed.

4.1. **Approximate separability of the Green's functions for fixed X, Y.**

1) X and Y are two disjoint compact domains in R^3, $\dim(X) = \dim(Y) = s = 3$. For two points $\mathbf{y}_1, \mathbf{y}_2 \in Y$, one can only claim $\alpha = 1$ in general. Since for any point $\mathbf{y} \in Y$ there is a solid cone with $\mathbf{y}$ as the vertex such that a segment of the ray (a straight line in homogeneous medium) connecting $\mathbf{y}$ and a point in the cone stays in X which gives a 1D curve of stationary phase (see Theorem 2.1). Since $\alpha = 1 < \frac{s}{2}$, Theorem 3.1, 3.3 give the lower bound $N_k^\epsilon \gtrsim k^2$ while Theorem 3.2, 3.4 give the upper bound $N_k^\epsilon \lesssim k^{3+\delta}$ for any $\delta > 0$.

2) X and Y are two disjoint compact surfaces in 3D, $\dim(X) = \dim(Y) = s = 2$. This is a typical scenario for boundary integral methods in which X and Y are two patches of the scattering boundaries. Generically, the ray going through two points $\mathbf{y}_1, \mathbf{y}_2 \in Y$ intersects X at most finite number of times, i.e., there are only isolated stationary points for the oscillatory surface integral $< \hat{G}(\cdot, \mathbf{y}_1), \hat{G}(\cdot, \mathbf{y}_2) >_X$. If there are isolated stationary points in the interior of X, $\alpha = \frac{s}{2}$, or if there are only isolated stationary points on the boundary ∂X, $\alpha = \frac{s+1}{2}$ (see Remark 2.3). For both cases, we have $\alpha \geq \frac{s}{2}$ and the following sharp estimates for k large enough from Theorem 3.1- 3.4

$$k^{2-\delta} \lesssim N_k^\epsilon \lesssim k^{2+\delta}, \quad \forall \delta > 0.$$

There are a few special setups belonging to this case when people compute the direct inverse of discretized linear systems for PDEs using the multi-frontal method in 3D. The full linear systems are reduced to smaller but dense linear systems corresponding to unknowns staying on planar subdomain boundaries, such as those depicted in Figure 8, after elimination of interior nodes in each subdomain. Further sparsifying these smaller but dense linear systems utilizing low rank approximations of off-diagonal submatrices is crucial for desiginning fast solvers. We use our approximate separability estimates for these typical setups to show why it is not doable for the Helmholtz equation in the high frequency limit, which has been observed widely in numerical computations. For $s = 2$, the upper bound is $N_k^\epsilon \lesssim k^{2+\delta}$ for any $\delta > 0$. For the lower bound, we first look at three typical configurations in homogeneous medium where rays are straight lines: (a) If X, Y are two disjoint coplanar regions as shown in Figure 8(a). For any point $\mathbf{y} \in Y$ there is a solid cone with $\mathbf{y}$ as the vertex such that a segment of the ray connecting $\mathbf{y}$ and a point in the cone stays in X. In this case we have $\alpha = \frac{1}{2}$ and $N_k^\epsilon \gtrsim k$ for k large enough; (b) If X, Y are two disjoint planar regions that are not coplanar nor parallel to each other, e.g. perpendicular to each other as shown in Figure 8(b), we have $\alpha = 1$ since the ray going through any two points $\mathbf{y}_1, \mathbf{y}_2 \in Y$ intersects X at most finite times (0 or 1). So one has $N_k^\epsilon \gtrsim k^{2-\delta}, \forall \delta > 0$ for k large enough; (c) If X, Y are two planar regions in parallel as shown in Figure 8(c), generically one has $\alpha = \frac{3}{2}$ since the ray going through any two points $\mathbf{y}_1, \mathbf{y}_2 \in Y$ does not intersect X (see Remark 2.3). So one has $N_k^\epsilon \gtrsim k^{2-\delta}, \forall \delta > 0$ for k large enough. If the medium is heterogeneous, a ray going through two points $\mathbf{y}_1, \mathbf{y}_2$ intersects a planar region X at most a finite number of times generically. So we have $\alpha \geq 1$ and the sharp low bound $N_k^\epsilon \gtrsim k^{2-\delta}, \forall \delta > 0$ in general no matter how they are positioned relatively. For a discretization with a fixed ratio between the grid size and the wavelength, the sharp lower bound means that the off-diagonal sub-matrices of the linear system after elimination of the interior nodes is of full rank modulo a constant in the high frequency limit.

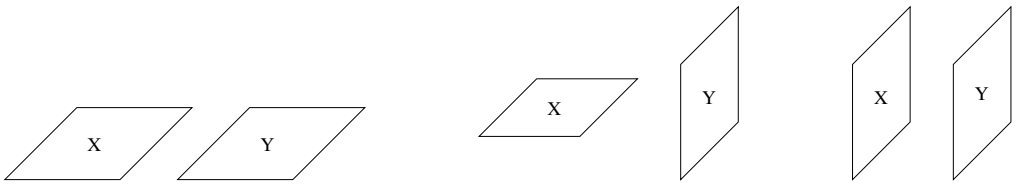

FIGURE 8. Two planar surfaces in 3D.

3) $X \in R^3$ is a compact domain ($\dim(X) = 3$), Y is a compact smooth curve ($\dim(Y) = s = 1$) or surface ($\dim(Y) = s = 2$) and X, Y are disjoint. Generically, given two points $\mathbf{y}_1, \mathbf{y}_2 \in Y$, depending on whether or not X contains a portion of the ray that goes through the two points, one has $\alpha = 1$ or $\alpha = 2$ respectively (see Theorem 2.1). Since $\alpha \geq \frac{s}{2}$, from Theorem 3.1- 3.4 one has the following sharp estimates for k large enough,

$$k^{s-\delta} \lesssim N_k^\epsilon \lesssim k^{s+\delta}, \quad \forall \delta > 0.$$

4) X is a 2D surface or 1D curve and Y is a 1D curve. Generically, a ray connection two points $\mathbf{y}_1, \mathbf{y}_2 \in Y$ intersects X at most finite number of time. Hence, we have $\alpha \geq 1$ if X is a surface and $\alpha \geq \frac{1}{2}$ if X is a curve using standard stationary phase theory. So for both cases we have sharp bounds for k large enough

$$k^{1-\delta} \lesssim N_k^\epsilon \lesssim k^{1+\delta} \quad \forall \delta > 0, \quad k \to \infty.$$

4.2. **Approximate separability of the Green's function for k dependent X, Y.** So far in this study we have shown that the lower bound for the number of terms, N_k^ϵ, in a separable approximation (2) of the Green's function $G(\mathbf{x}, \mathbf{y})$ of the Helmholtz equation in the high frequency limit grows at least with certain power of k (Theorem 3.1, 3.3) in general. However, there are special k *dependent* setups of X and Y for which high separability of the Green's function of the Helmholtz equation can be achieved in the high frequency limit, i.e., N_k^ϵ does not depend on k and depends on ϵ logarithmically. These special setups can be exploited to develop fast algorithms in practice by utilizing low rank approximations.

Assume that the geometric optics Ansatz $G(\mathbf{x}, \mathbf{y}) = A(\mathbf{x}, \mathbf{y}) e^{ik\phi(\mathbf{x},\mathbf{y})}$ is valid, where $A(\mathbf{x}, \mathbf{y})$ and $\phi(\mathbf{x}, \mathbf{y})$ are the smooth amplitude and phase functions respectively. To achieve high separability in these special k dependent setups, one has to avoid rapid change in the phase function which causes the fast decorrelation between two Green's functions. A typical strategy is to find $\phi_1(\mathbf{x})$ and $\phi_2(\mathbf{y})$ such that $k(\phi(\mathbf{x}, \mathbf{y}) - \phi_1(\mathbf{x}) - \phi_2(\mathbf{y}))$ is uniformly bounded with respect to $\mathbf{x} \in X, \mathbf{y} \in Y$ and k since the amplitude function $A(\mathbf{x}, \mathbf{y})$ is independent of k. Then a high separable approximation is possible for $e^{ik(\phi(\mathbf{x},\mathbf{y}) - \phi_1(\mathbf{x}) - \phi_2(\mathbf{y}))}$ due to the fast convergence of Taylor expansion for e^{ikz} for $|z| \leq C < \infty$. The phase difference between two Green's functions at different sources $\mathbf{y}_1, \mathbf{y}_2$ can be written as

$$\begin{aligned} & k(\phi(\mathbf{x}, \mathbf{y}_1) - \phi(\mathbf{x}, \mathbf{y}_2)) \\ =& k(\phi_2(\mathbf{y}_1) - \phi_2(\mathbf{y}_2)) + k[(\phi(\mathbf{x}, \mathbf{y}_1) - \phi_1(\mathbf{x}) - \phi_2(\mathbf{y}_1)) - (\phi(\mathbf{x}, \mathbf{y}_2) - \phi_1(\mathbf{x}) - \phi_2(\mathbf{y}_2))], \end{aligned}$$

which is a constant phase shift $k(\phi_2(\mathbf{y}_1) - \phi_2(\mathbf{y}_2))$ plus a term that is bounded uniformly with respect to $\mathbf{x} \in X, \mathbf{y} \in Y$ and k . Hence no fast oscillation is present to decorrelate two Green's functions. For simplicity the 3D free space Green's function (7) of the Helmholtz equation is used for illustration in the following examples.

1) A trivial case where X, Y are two line segments that are collinear as shown in Figure 9(a) in a homogeneous medium

$$< \hat{G}_0(\cdot, \mathbf{y}_1), \hat{G}_0(\cdot, \mathbf{y}_2) >= \frac{1}{\|G_0(\cdot, \mathbf{y}_1)\|_2 \|G_0(\cdot, \mathbf{y}_2)\|_2} e^{ik(\mathbf{y}_2 - \mathbf{y}_1)} \int_X \frac{1}{|\mathbf{x} - \mathbf{y}_1||\mathbf{x} - \mathbf{y}_2|} d\mathbf{x}. \tag{99}$$

Denote the axis going through these two line segments as r, we have

$$G_0(\mathbf{x}, \mathbf{y}) = \frac{1}{4\pi} \frac{e^{-ik(r_\mathbf{x} - r_\mathbf{y})}}{r_\mathbf{y} - r_\mathbf{x}} = \frac{1}{4\pi} e^{-ikr_\mathbf{x}} e^{ikr_\mathbf{y}} r_\mathbf{y}^{-1} \sum_{m=0}^{\infty} (\frac{r_\mathbf{x}}{r_\mathbf{y}})^m. \tag{100}$$

In this trivial case, $\phi(\mathbf{x}, \mathbf{y}) = \phi_1(\mathbf{x}) + \phi_2(\mathbf{y})$, where $\phi_1(\mathbf{x}) = -r_\mathbf{x}, \phi_2(\mathbf{y}) = r_\mathbf{y}$. It is easy to see that the geometric series can be truncated at $[(\log \frac{l_X}{l_X + \rho})^{-1} \log(4\pi\rho\epsilon)] + 1$ to get a

separable approximation for any $\epsilon > 0$ independent of k, where l_X is the length of X and ρ is the distance between X and Y. So we have

$$N_k^\epsilon \leq [\max\{(\log \frac{l_X}{l_X+\rho})^{-1}, (\log \frac{l_Y}{l_Y+\rho})^{-1}\} \log(4\pi\rho\epsilon)] + 1.$$

The same argument can be applied to two disjoint curve segments X and Y that lie on the same ray in a heterogeneous medium. In this case

$$< \hat{G}(\cdot, \mathbf{y}_1), \hat{G}(\cdot, \mathbf{y}_2) >= \frac{1}{\|G(\cdot, \mathbf{y}_1)\|_2 \|G(\cdot, \mathbf{y}_2)\|_2} e^{ik\phi(\mathbf{y}_1, \mathbf{y}_2)} \int_X A(\mathbf{x}, \mathbf{y}_1) A(\mathbf{x}, \mathbf{y}_2) d\mathbf{x}, \tag{101}$$

where $\phi(\mathbf{y}_1, \mathbf{y}_2)$ is the travel time between $\mathbf{y}_1$ and $\mathbf{y}_2$ and $A(\mathbf{x}, \mathbf{y}_1), A(\mathbf{x}, \mathbf{y}_2)$ are the corresponding amplitudes in a geometric optics Ansatz discussed in Section 2.2.

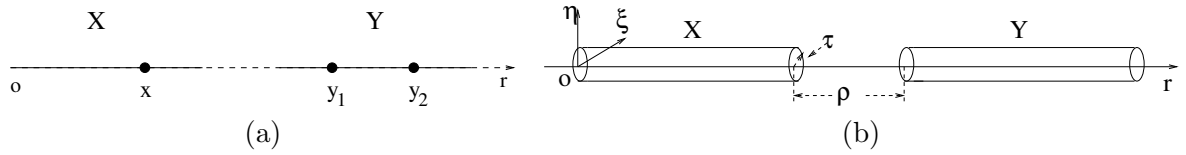

FIGURE 9. Two special k dependent setups of X and Y that allow highly separabilility of the Green's function.

2) X and Y are two disjoint thin cylinders around a line in a homogeneous medium as shown in Figure 9(b). The lengths of the two cylinders can be of $O(1)$. However, the radius of the two cylinders have to be of $O(k^{-1})$ and the separation distance between X and Y is larger than the radius of the two cylinders. This 3D setup is analogous to the 2D setup in [23]. Numerical verification will be presented in Section 5.

Let the longitudinal axis be r and the other two orthogonal coordinates in the plane perpendicular to r be ξ, η. Let $\mathbf{x} = (r_x, \xi_x, \eta_x) \in X$ and $\mathbf{y} = (r_y, \xi_y, \eta_y) \in Y$. Denote $\rho = \inf_{\mathbf{x}\in X, \mathbf{y}\in Y}(r_x - r_y)$ and $\tau = \sup_{\mathbf{x}\in X, \mathbf{y}\in Y} \sqrt{\xi^2 + \eta^2}$. Assume $k\tau < \frac{1}{2}, \mu = \frac{\tau}{\rho} < \frac{1}{2}$. Again in this case $\phi_1(\mathbf{x}) = -r_x, \phi_2(\mathbf{y}) = r_y$ as in the previous case. One has

$$k|\phi(\mathbf{x}, \mathbf{y}) - \phi_1(\mathbf{x}) - \phi_2(\mathbf{y})| = k(|\mathbf{x} - \mathbf{y}| - (r_y - r_x)) < 2k\tau = 1$$

Next, we give an explicit separable approximation using asymptotic expansions.

(102)

$$k|\mathbf{x} - \mathbf{y}| = k\sqrt{(r_x - r_y)^2 + (\xi_x - \xi_y)^2 + (\eta_x - \eta_y)^2}$$

$$= k(r_y - r_x) + k\sqrt{(\xi_x - \xi_y)^2 + (\eta_x - \eta_y)^2} \sum_{m=1}^{\infty} \frac{(-1)^m (2m)!}{(1-2m)(m!)^2 4^m} \frac{((\xi_x - \xi_y)^2 + (\eta_x - \eta_y)^2)^{m-1/2}}{(r_y - r_x)^{2m-1}}.$$

Note that $k\sqrt{(\xi_x-\xi_y)^2+(\eta_x-\eta_y)^2}\le 2k\tau<1$ and $\frac{(-1)^m(2m)!}{(1-2m)(m!)^2 4^m}<\frac{1}{2m}$. The second term in the above expression can be bounded by a geometric series $\sum_{m=1}^{\infty}(\frac{2\tau}{\rho})^{2m-1}$. So we have

(103)
$$< \hat{G}_0(\cdot,\mathbf{y}_1), \hat{G}_0(\cdot,\mathbf{y}_2) >= \frac{1}{\|G_0(\cdot,\mathbf{y}_1)\|_2\|G_0(\cdot,\mathbf{y}_2)\|_2} e^{ik(r_{y_1}-r_{y_2})}\int_X \frac{e^{i\tilde{\phi}(\mathbf{x})}}{|\mathbf{x}-\mathbf{y}_1||\mathbf{x}-\mathbf{y}_2|}d\mathbf{x},$$

where $\tilde{\phi}(\mathbf{x})=k[(|\mathbf{x}-\mathbf{y}_1|-(r_{y_1}-r_x))-(|\mathbf{x}-\mathbf{y}_2|-(r_{y_2}-r_x))]$ and $|\tilde{\phi}(\mathbf{x})|=O(1), \forall \mathbf{x}\in X, \forall \mathbf{y}_1,\mathbf{y}_2\in Y$. Again no fast oscillation due to rapid change of phase is present in the integral. We show an explicit separable approximation based on the expansion (102).

For any tolerance $\epsilon>0$, take q such that $(\frac{2\tau}{\rho})^{2q+1}(1-\frac{2\tau}{\rho})^{-1}<\epsilon$. So only the first $q=O(|\log\epsilon|)$ terms are needed in the summation in (102). Denote $Q(\mathbf{x},\mathbf{y})$ to be the first q term expansion,

$$Q(\mathbf{x},\mathbf{y})=k\sqrt{(\xi_x-\xi_y)^2+(\eta_x-\eta_y)^2}\sum_{m=1}^{q}\frac{(-1)^m(2m)!}{(1-2m)(m!)^2 4^m}\frac{((\xi_x-\xi_y)^2+(\eta_x-\eta_y)^2)^{m-1/2}}{(r_y-r_x)^{2m-1}}.$$

$Q(\mathbf{x},\mathbf{y})$ is bounded independent of k and so

$$e^{ik|\mathbf{x}-\mathbf{y}|}=e^{ik(r_y-r_x)}e^{i(Q(\mathbf{x},\mathbf{y})+\epsilon)}=e^{ik(r_y-r_x)}e^{iQ(\mathbf{x},\mathbf{y})}+O(\epsilon).$$

Since e^x has a $p=O(|\log\epsilon|)$ term polynomial expansion for any tolerance ϵ for a bounded x, we have

$$e^{iQ(\mathbf{x},\mathbf{y})}=\sum_{l=0}^{p}\frac{[iQ(\mathbf{x},\mathbf{y})]^l}{l!}+O(\epsilon).$$

Each term in the expansion of $[Q(\mathbf{x},\mathbf{y})]^l$ is like

$$\left[k\sqrt{(\xi_x-\xi_y)^2+(\eta_x-\eta_y)^2}\right]^l\frac{\left(\sqrt{(\xi_x-\xi_y)^2+(\eta_x-\eta_y)^2}\right)^m}{(r_y-r_x)^m}$$

where the integer m ranges from l to $(2q-1)l$ and $m+l$ is even. One only needs to keep those $m\le 2q$ terms in the expansion because $(\frac{2\tau}{\rho})^{2q+1}=O(\epsilon)$ and $k\sqrt{(\xi_x-\xi_y)^2+(\eta_x-\eta_y)^2}<1$. So altogether we have $O(pq)=O(|\log\epsilon|^2)$ terms of the form

(104)
$$\frac{((\xi_x-\xi_y)^2+(\eta_x-\eta_y)^2)^m}{(r_y-r_x)^l},$$

where $0<l\le m\lesssim|\log\epsilon|$ are integers. Each term

$$((\xi_x-\xi_y)^2+(\eta_x-\eta_y)^2)^m=[(\xi_x^2+\eta_x^2)-2\xi_x\xi_y-2\eta_x\eta_y+(\xi_y^2+\eta_y^2)]^m$$

can be expanded into $\frac{(m+3)!}{m!3!}=O(|\log\epsilon|^3)$ separable terms. Further more, since $r_x>r_y\ge 0$, $O(|\log\epsilon|)$ leading terms are needed in the following expansion to have an ϵ approximation,

(105)
$$(r_y-r_x)^{-l}=r_x^{-l}\left[1-\sum_{m=1}^{\infty}\left(\frac{r_y}{r_x}\right)^m\right]^l.$$

Hence a separable ϵ-approximation of $e^{ik|\mathbf{x}-\mathbf{y}|}$ requires $O(|\log\epsilon|^6)$ terms. The last term we need to make a separable approximation is $\frac{1}{|\mathbf{x}-\mathbf{y}|}$.

$$\frac{1}{|\mathbf{x}-\mathbf{y}|} = (r_y - r_x)^{-1}\left[1+\frac{(\xi_x-\xi_y)^2+(\eta_x-\eta_y)^2}{(r_x-r_y)^2}\right]^{-\frac{1}{2}}$$

$$= r_x^{-l}\left[1-\sum_{m=1}^{\infty}\left(\frac{r_y}{r_x}\right)^m\right]^l\left[1+\sum_{m=1}^{\infty}\frac{(-1)^m(2(m+1))!}{2(2m+1)((m+1)!)^2 4^m}\frac{((\xi_x-\xi_y)^2+(\eta_x-\eta_y)^2)^m}{(r_y-r_x)^{2m}}\right]$$

Both summations in the above the formula can be truncated at $O(|\log\epsilon|)$ terms with ϵ error. Each term in the summation in the second bracket is similar to the term in (104) which can be approximated by at most $O(|\log\epsilon|^4)$ separable terms. So $\frac{1}{|\mathbf{x}-\mathbf{y}|}$ can also be approximated by $O(|\log\epsilon|^6)$ separable terms. Combine all these terms together we have $N_k^\epsilon \le O(|\log\epsilon|^{12})$ for this setup.

3) Here we study two k dependent setups of X and Y that have been proposed and used for developing fast algorithms.

(a) In [26, 7, 19] fast butterfly algorithms for computing highly oscillatory Fourier integral operators and boundary integrals for the Helmholtz equation were developed. The key idea is a dyadic decomposition of two domains A, B into tree structures T_A, T_B, from root to leaf, and a recursive paring of $X \in T_A$ and $Y \in T_B$ such that the phase function or the kernel function for the boundary integrals, i.e., the free space Green's function, restricted on $X \times Y$ has high separability or low rank approximation in discrete setting. The condition for pairing X and Y is that the product of the diameters of X and Y is less than or equal to $\frac{1}{k}$. For this setup, the key observation is that one can construct a simple separable phase function, $\phi(\mathbf{x}_0,\mathbf{y})+\phi(\mathbf{x},\mathbf{y}_0)-\phi(\mathbf{x}_0,\mathbf{y}_0)$ that can approximate the original phase function uniformly well, i.e., $k|\phi(\mathbf{x},\mathbf{y})-\phi(\mathbf{x}_0,\mathbf{y})-\phi(\mathbf{x},\mathbf{y}_0)+\phi(\mathbf{x}_0,\mathbf{y}_0)|$ is uniformly bounded for all k, $\mathbf{x}\in X, \mathbf{y}\in Y$, where $\mathbf{x}_0, \mathbf{y}_0$ are the centers of X, Y respectively. Under an analytic function assumption for $\phi(\mathbf{x},\mathbf{y})$, $k(\phi(\mathbf{x},\mathbf{y})-\phi(\mathbf{x}_0,\mathbf{y})-\phi(\mathbf{x},\mathbf{y}_0)+\phi(\mathbf{x}_0,\mathbf{y}_0))$ can be approximated by a Taylor expansion with $O(|\log\epsilon|)$ terms (see the proof in [7]).

(b) In [9] fast directional multilevel algorithms for integrals were developed based on directional low rank approximations of the free space Green's functions of the Helmholtz equation on two domains X_r and Y_r that satisfy a directional parabolic separation condition: Y_r is a ball of radius r centered at a point c and X_r is a domain containing points that are at a distance r^2 or greater from c and belong to a cone centered at c with spanning angle $\frac{1}{r}$. Here r is a length scale in the unit of wavelength $\lambda = \frac{2\pi}{k}$. For this setup, the phase function $|\mathbf{x}-\mathbf{y}| = \frac{k}{2\pi}|\lambda\mathbf{x}-\lambda\mathbf{y}|$ can be uniformly approximated by $\hat{\mathbf{x}}\cdot(\mathbf{x}-\mathbf{y}) = |\mathbf{x}| - \hat{\mathbf{x}}\cdot\mathbf{y} = |\mathbf{x}| - (\hat{\mathbf{x}}-\hat{l})\cdot\mathbf{y} - \hat{l}\cdot\mathbf{y}$ which can be further approximated by $|\mathbf{x}| - \hat{l}\cdot\mathbf{y}$ uniformly, where $\hat{\mathbf{x}} = \frac{\mathbf{x}}{|\mathbf{x}|}$ and $\hat{l}$ is the direction the cone centered at. In other words, let $\phi(\mathbf{x},\mathbf{y}) = |\mathbf{x}-\mathbf{y}|$ and $\phi_1(\mathbf{x}) = |\mathbf{x}|, \phi_2(\mathbf{y}) = -\hat{l}\cdot\mathbf{y}$, then $|\phi(\mathbf{x},\mathbf{y})-\phi_1(\mathbf{x})-\phi_2(\mathbf{y})|$ is uniformly bounded and has an $O(\log|\epsilon|)$ term separable approximation with error $\epsilon > 0$.

4) Here we present a scaling argument to show a k dependent asymptotic setup for two disjoint domains, X and Y, for which high separability of the Green's function of the Helmholtz equation in the high frequency limit exists. Then we use this scaling argument to show that the condition for the setup of butterfly algorithm is tight.

Let r_X, r_Y denote the diameters of X, Y respectively. Denote the distance between X and Y to be $dist(X,Y)$. Without loss of generality, let $r_Y \leq r_X$ and $r_X = O(1)$. Actually the size of X is not restricted since it can always be scaled to $O(1)$ by scaling $\mathbf{x}$ to $\frac{\mathbf{x}}{r_X}$ and k to $r_X k$ for the Helmholtz equation (3). Assume $r_Y \ll dist(X,Y)$. From the scaling argument in Remark 2.2, the rate of decorrelation of two Green's functions is rescaled to $\left| < \hat{G}(\cdot, \mathbf{y}_1), \hat{G}(\cdot, \mathbf{y}_2) > \right| \lesssim \left(\frac{|\mathbf{y}_1 - \mathbf{y}_2|^2 k}{dist(X,Y)} \right)^{-\alpha}, \forall \mathbf{y}_1, \mathbf{y}_2 \in Y$ for some $\alpha > 0$. So if $r_Y \lesssim \sqrt{\frac{dist(X,Y)}{k}}$, there is no fast decorrelation of two Green's functions. On the other hand, if $r_Y \gtrsim \sqrt{\frac{dist(X,Y)}{k^{1-\delta}}}, \forall \delta > 0$, one can put a grid with a grid size a little larger than $\sqrt{\frac{dist(X,Y)}{k}}$ in Y so that they become more and more decorrelated as $k \to \infty$. At the same time, the number of grid points in Y becomes larger and larger as $k \to \infty$. Use a similar argument as in Lemma 3.1 one can show a lower bound estimate for the approximate separability which grows with some power of k. The above discussion can include $dist(X,Y)$ as well. For example, if $dist(X,Y) = O(k)$, r_Y can be $O(1)$.

In a typical setup for the butterfly algorithm [26, 7, 19], there are two domains A, B whose sizes are of $O(1)$ and $dist(A,B) = O(1)$. For example, A, B may be disjoint patches on the boundaries of scatterers in boundary integral methods. Dyadic decomposition of A, B gives tree structures T_A, T_B with $L = O(\log k)$ levels, where the roots are A, B and the leaf nodes at level L are of sizes comparable to the wavelength $\lambda = O(k^{-1})$. Then the interaction between A and B through a highly oscillatory kernel function, e.g., the Green's function of the Helmholtz equation or a Fourier integral operator, is computed based on a recursive pairing of nodes X, $A \supseteq X \in T_A$, and Y, $B \supseteq Y \in T_B$, such that the level of X, $l(X)$, and the level of Y, $l(Y)$, satisfy $l(X) + l(Y) = L$. The key observation is that the interaction between X and Y has a low rank approximation. It was shown in [7] that the low rank approximation is guaranteed if $r_X r_Y = O(k^{-1})$ which is implied by the condition $l(X) + l(Y) = L$ (plus some analyticity condition on the phase function). It can be easily seen that high separability for the setup for the butterfly algorithm falls into the asymptotic regime discussed above. The requirement of analyticity of the phase function is guaranteed by the condition $dist(X,Y) \geq dist(A,B) = O(1)$. The condition $r_X r_Y = O(k^{-1})$ implies that the smaller domain Y (or X) satisfies r_Y(or r_X)$\leq O(k^{-\frac{1}{2}})$. In particular, this condition is tightly satisfied when $r_X \sim r_Y$ or $l(X) = l(Y)$. If $r_A r_B = O(k^{\delta})$ for any $\delta > 0$ or $dist(A,B) \to 0$ as $k \to \infty$, then the condition is violated. Then high separability (or low rank approximation for discrete system) is not valid as discussed above.

4.3. **Approximate separability of the Green's functions of the Helmholtz equation with boundary conditions.** So far we have shown approximate separability estimates for the Green's function of the Helmholtz equation in the high frequency limit in the

whole space. Here we study an example in which boundary reflections are present. First we study the approximate separability for the Green's function of the Helmholtz equation in half space with a homogeneous Dirichlet boundary condition as illustrated in Figure 10(a). The Green's function for the upper space, denoted by $G_1(\mathbf{x},\mathbf{y})$, can be explicitly constructed from the free space Green's function, denoted by $G_0(\mathbf{x},\mathbf{y})$,

$$G_1(\mathbf{x},\mathbf{y}) = G_0(\mathbf{x},\mathbf{y}) - G_0(\mathbf{x},\overline{\mathbf{y}}),$$

where $\overline{\mathbf{y}}$ is the mirror image of $\mathbf{y}$ with respect to the boundary. Decorrelation of G_1 can be deduced from that of G_0. Given two disjoint compact domains X and Y in the upper half space and two points $\mathbf{y}_1, \mathbf{y}_2 \in Y$, if the line connecting these two points, denoted by $l^{\mathbf{y}_2}_{\mathbf{y}_1}$, intersects with X, or none of the the lines $l^{\overline{\mathbf{y}}_2}_{\mathbf{y}_1}$, $l^{\mathbf{y}_2}_{\overline{\mathbf{y}}_1}$, $l^{\overline{\mathbf{y}}_2}_{\overline{\mathbf{y}}_1}$ intersects with X, $< G_0(\cdot,\mathbf{y}_1), G_0(\cdot,\mathbf{y}_2) >$ is the dominant term in the following and we have

(106)

$$\begin{aligned}
&|< G_1(\cdot,\mathbf{y}_1), G(\cdot,\mathbf{y}_2) >| \\
&= |<G_0(\mathbf{x},\mathbf{y}_1), G_0(\mathbf{x},\mathbf{y}_2)> - <G_0(\mathbf{x},\mathbf{y}_1), G_0(\mathbf{x},\overline{\mathbf{y}}_2)> - <G_0(\mathbf{x},\overline{\mathbf{y}}_1), G_0(\mathbf{x},\mathbf{y}_2)> + <G_0(\mathbf{x},\overline{\mathbf{y}}_1), G_0(\mathbf{x},\overline{\mathbf{y}}_2)>| \\
&\sim |< G_0(\cdot,\mathbf{y}_1), G_0(\cdot,\mathbf{y}_2) >|,
\end{aligned}$$

since $|\mathbf{y}_1 - \mathbf{y}_2| \le \min(|\mathbf{y}_1 - \overline{\mathbf{y}}_2|, |\overline{\mathbf{y}}_1 - \mathbf{y}_2|, |\overline{\mathbf{y}}_1 - \overline{\mathbf{y}}_2|)$ and $dist(\mathbf{y}_j, X) < dist(\overline{\mathbf{y}}_j, X), j = 1, 2$. Otherwise, decorrelation of $G_1(\mathbf{x},\mathbf{y}_1)$ and $G_1(\mathbf{x},\mathbf{y}_2)$ may be slower than that of $G_0(\mathbf{x},\mathbf{y}_1)$ and $G_0(\mathbf{x},\mathbf{y}_2)$. In general, for two disjoint compact domains X and Y, there is a solid cone at each point $\mathbf{y} \in Y$ with $\mathbf{y}$ as the vertex such that a line connecting $\mathbf{y}$ and any other point in the cone intersects X. The correlation between two Green's functions with one source at $\mathbf{y}$ and the other source in the cone with or without the boundary is of the same order from (106). Due to the presence of line of stationary points, these stronger correlations are the leading terms in the estimate of $tr(A^T A)$ as discussed in Remark 3.3. Hence the proof and results in Lemma 3.1 and those lower bound estimates in Theorem 3.1 and Theorem 3.3 for the approximate separability of the free space Green's function of the Helmholtz equation in the high frequency limit hold for the case with a reflection boundary too. It is also easy to see that a separable approximation of the Green's function $G_1(\mathbf{x},\mathbf{y})$ for $\mathbf{x} \in X, \mathbf{y} \in Y$ can be obtained by combining separable approximations of $G_0(\mathbf{x},\mathbf{y})$ for $\mathbf{x} \in X, \mathbf{y} \in Y$ and that of $G_0(\mathbf{x},\overline{\mathbf{y}})$ for $\mathbf{x} \in X, \overline{\mathbf{y}} \in \overline{Y}$, where $\overline{Y}$ is the mirror image of Y with respect to the boundary. So the upper bound estimates in Theorem 3.2 and Theorem 3.4 also hold.

Although the asymptotic estimates for the lower bound and upper bound for the approximate separability of the Green's functions of the Helmholtz equation in the case with a boundary are of the same order to those in free space, the least number of terms, N_k^ϵ, needed for a separable approximation for the Green's function for a fixed $\epsilon > 0$ may increase due to the reflections at the boundary in general. Because the Green's function $G_1(\mathbf{x},\mathbf{y})$ viewed as a family function in X parameterized by $\mathbf{y} \in Y$ is composed of a family of free space Green's function $G_0(\mathbf{x},\mathbf{y})$ with $\mathbf{y}$ in a larger domain, $\mathbf{y} \in Y \cup \overline{Y}$. Geometrically, there are multiple rays instead of one ray connecting any two points $\mathbf{x} \in X$ and $\mathbf{y} \in Y$ with the presence of a reflection boundary. The phase function becomes more complicated

and needs more terms in a separable approximation. In general, one can expect that the presence of multiple scatterings can cause faster decorrelation of the Green's functions and hence the increase of N_k^ϵ. As the distance from the boundary to X and Y becomes larger and larger, the effect from the boundary becomes less and less.

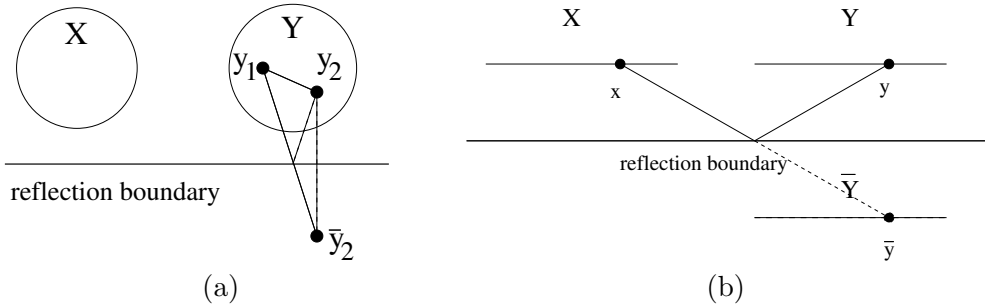

FIGURE 10. Half space setups with a reflection boundary.

Here, we apply the above study of boundary effects to a particular setup as depicted in Figure 10(b). Here X and Y are two disjoint collinear line segments parallel to the boundary. In free space, $G_0(\mathbf{x},\mathbf{y}), \mathbf{x} \in X, \mathbf{y} \in Y$ is highly separable as discussed in the first special case in Section 4.2. Now suppose there is a reflection boundary whose distance to X, Y is less than a wavelength and than the separation distance between X and Y. Since the Green's function with the boundary is composed of two free space Green's functions, $G_1(\mathbf{x},\mathbf{y}) = G_0(\mathbf{x},\mathbf{y}) - G_0(\mathbf{x},\overline{\mathbf{y}})$, where $\overline{\mathbf{y}}$ is the mirror image of $\mathbf{y}$ with respect to the boundary, it follows from the case study for two thin cylinders in Section 4.2 or study in [23, 10] that $G_1(\mathbf{x},\mathbf{y}), \mathbf{x} \in X, \mathbf{y} \in Y$ is highly separable for this setup. This is the key observation for the low rank approximation used in the sweeping preconditioner for the Helmholtz equation in 2D in [10]. However, this highly separable property does not hold if the boundary is of fixed distance to X, Y as $k \to \infty$. Neither does high separability hold in an analogous setup in 3D where X, Y are planar regions. As discussed in case 2) in Section 4.1, even for two fixed disjoint compact co-planar 2D regions without the boundary, N_k^ϵ is at least of $O(k)$ for a homogeneous medium and is of $O(k^{2-\delta}), \forall \delta > 0$, in general as $k \to \infty$.

5. Numerical tests

Here we present a few numerical examples to corroborate our analysis in previous sections. In all our numerical examples the free space Green's functions in 2D and 3D are used. Our computational grid size h resolves the wavelength $\lambda = 2\pi/k$, $h = \lambda/15$ in 2D and $h = \lambda/13$ in 3D.

Example 1. We show the correlation between two normalized free space Green's functions, $\left| < \hat{G}_0(\cdot,\mathbf{y}_1), \hat{G}_0(\cdot,\mathbf{y}_2) >_X \right|$, in 2D and 3D, where X is a compact domain. In this test, we show results for k starting from 50 with an increment of 5.

Figure 11 shows the correlation between two free space Green's functions in 2D. Here the domain X is a disc centered at $(0,0)$ with radius 0.4. For the results shown in Figure 11(a)

the two points $\mathbf{y}_1, \mathbf{y}_2$ lie on x-axis outside X. The line going through $\mathbf{y}_1, \mathbf{y}_2$ intersects X and the segment of intersection is a line of stationary points for $< \hat{G}_0(\cdot, \mathbf{y}_1), \hat{G}_0(\cdot, \mathbf{y}_2) >_X$. For the results shown in Figure 11(b), the line going through $\mathbf{y}_1, \mathbf{y}_2$ is parallel to y-axis and does not intersect X. Hence there is no stationary point for $< \hat{G}_0(\cdot, \mathbf{y}_1), \hat{G}_0(\cdot, \mathbf{y}_2) >_X$. As shown in the proof of Theorem 2.1, two Green's functions in this case decorrelate much faster than the afore mentioned case as $k \to \infty$. All results show that two Green's functions decorrelate faster when $|\mathbf{y}_1 - \mathbf{y}_2|$ becomes larger as shown by Theorem 2.1. It can also be seen that as $\mathbf{y}_1, \mathbf{y}_2$ are further away from X, two Green's functions become more correlated due to the scaling of the gradient and the Hessian of the phase function in term of the distance from $\mathbf{y}_1, \mathbf{y}_2$ to X as explained in Remark 2.2.

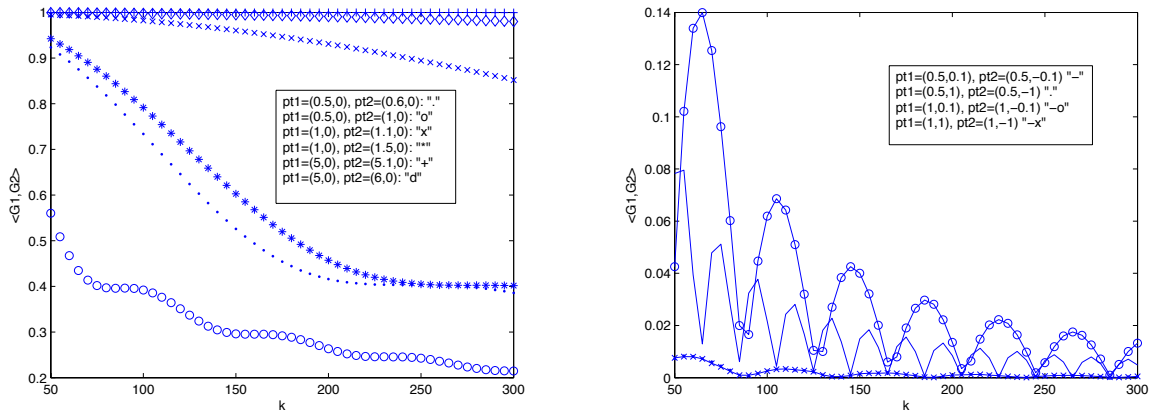

(a) (b)

FIGURE 11. Correlation between two normalized free space Green's functions in 2D.

Figure 12 shows the boundary effect with a homogeneous Dirichlet boundary condition. The boundary is an infinite line that is parallel to x-axis located at $y = -d$. For the results shown in Figure 12(a), X is again a disc as before. One can see that the boundary condition does affect the correlation between two Green's functions. However, the asymptotic behavior is similar to the one without boundary condition as $k \to \infty$. For results in Figure 12(b), X is a line segment on x-axis between $[-0.5, 0.5]$, which is co-linear with the two points $\mathbf{y}_1, \mathbf{y}_2$. Without the boundary, the two Green's functions have a constant difference in their phases and hence are highly correlated. When the boundary is present but not too close or too far from $\mathbf{y}_1, \mathbf{y}_2$ and X, we do see less correlation due to the boundary effect. When the boundary is either very close or the boundary is very far, the two Green's functions become highly correlated as explained in Section 4.3.

Figure 13 shows corresponding tests in 3D. The behavior in 3D is similar to those in 2D. The domain X is a ball centered at the origin with radius 0.4. For the results shown in Figure 13(a), the two points $\mathbf{y}_1, \mathbf{y}_2$ lie on x-axis outside X. The line going through $\mathbf{y}_1, \mathbf{y}_2$

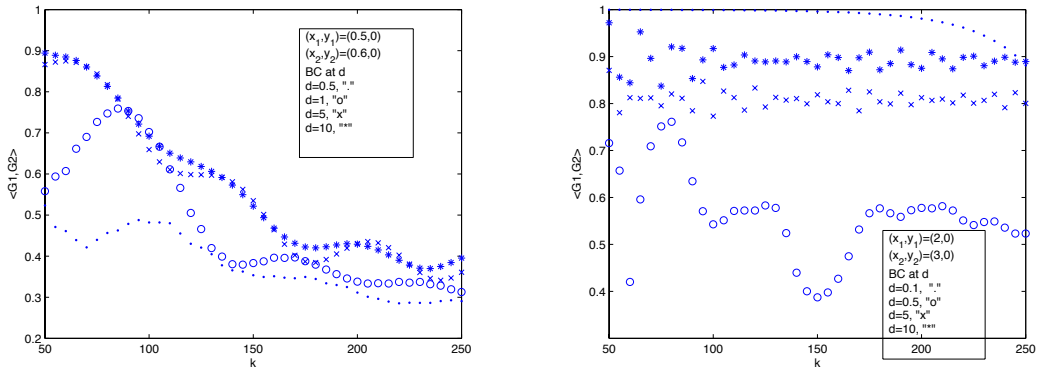

(a) (b)

FIGURE 12. Correlation between two normalized Green's functions in 2D with boundary effect.

intersects X and the two Green's functions decorrelate relatively slow. For the same setup, Figure 13(b) shows the effect of a Dirichlet boundary condition.

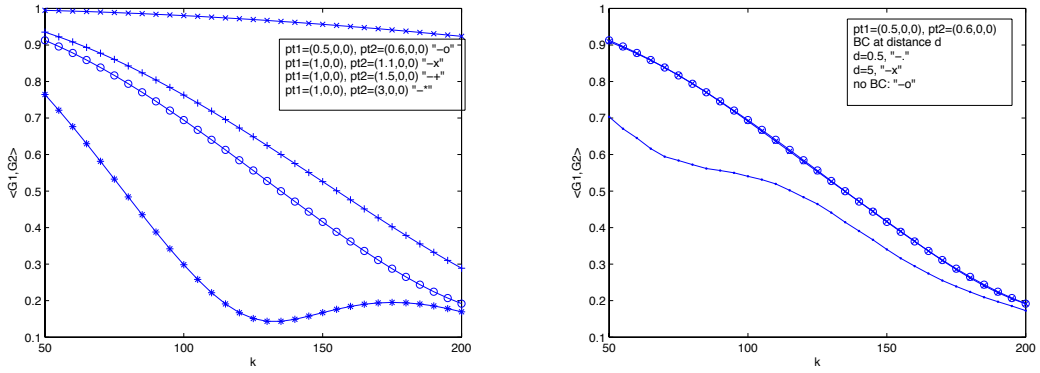

(a) (b)

FIGURE 13. Correlation between two normalized Green's functions in 3D.

Example 2 Here we present the pattern of singular values for the matrix $G(\mathbf{x}_i, \mathbf{y}_j)$, where $\mathbf{x}_i$ and $\mathbf{y}_j$ are uniformly distributed grid points in X and Y respectively with a grid size that resolves the wavelength. The 3D free space Green's function is used in the tests. In these tests, we show results for k ranging from 10 to 150 with an increment of 5. In the following figures, the solid lines show the number of leading singular values that is larger than ϵ vs. the wave number k while the dotted lines show $\underline{N}_k^\epsilon$ defined in Definition 3.2. In all tests we use three threshold values $\epsilon = 10^{-2}, 10^{-4}, 10^{-6}$.

Figure 14(a) shows the result for two line segments that are perpendicular to each other: $X = \{(x, y, z)|x \in [-0.5, 0.5], y = 0, z = 0\}$ and $Y = \{(x, y, z)|x = 0, y = 0.2, z \in [-0.5, 0.5]\}$. Figure 14(b) shows the result for X, a sphere centered at origin with radius 0.5, and $Y = \{(x, y, z)|x \in [0.6, 1.6], y = 0.6, z = 0\}$. As studied in Section 4.1 case 4), a linear growth of N_k^ϵ in k is expected.

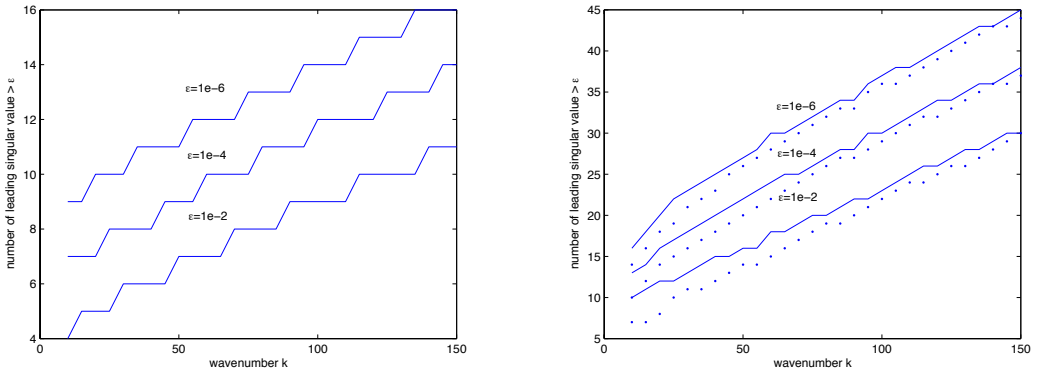

FIGURE 14. Leading singular values vs. wave number for $\dim(Y) = 1$.

Figure 15 shows the result for two planar squares X, Y of length 0.4 for each side. The relative positions of X and Y corresponds to the three setups as discussed in Section 4.1 case 2) and demonstrated in Figure 8. Figure 15(a) shows the results for X, Y that are side by side and coplanar with a distance 0.1 between them. Figure 15(b) shows the results for X, Y that are side by side and orthogonal to each other with a distance 0.1 between them. Figure 15(c) shows the results for X, Y that are side by side in parallel with a distance 0.3 between them. As analyzed in Section 4.1, setup (a) has the slowest rate of decorrelation between two Green's functions and hence also the slowest growth of N_k^ϵ while case (c) has the fastest rate of decorrelation between two Green's functions and hence also the fastest growth of N_k^ϵ among the three setups as $k \to \infty$. At least linear growth is observed in setup (a). In both setups (b) and (c) a quadratic growth, as predicted by the sharp lower bound and upper bound estimates analyzed in Section 4.1 case 2), is observed. If the medium is heterogeneous, linear growth of N_k^ϵ in setup (a) may not be observed since the ray going through two points $\mathbf{y}_1, \mathbf{y}_2 \in Y$ does not have a segment staying in X (a curve of stationary points) in general as discussed in Section 4.1 case 2).

Figure 16(a) shows an example of two spheres of radius 0.2 with a separation distance of 0.2 between them. At the maximum wave number $k = 150$, 20,000 points are randomly distributed on the surface of each sphere. For smaller wave numbers, the number of points are proportional reduced. Again one sees that the number of leading singular values grows quadratically as predicted by the study in Section 4.1 for case 2). Figure 16(b) shows an example of two thin cylinders as illustrated in Figure 9(b). The radius of each cylinder is

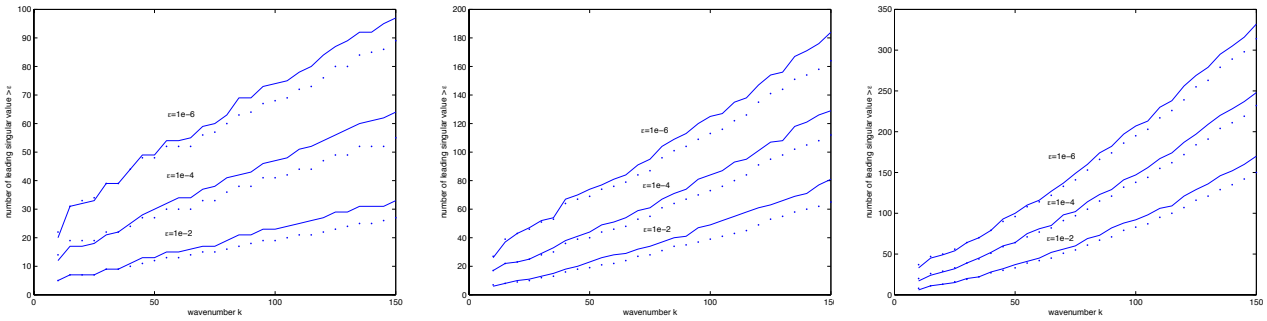

(a) (b) (c)

FIGURE 15. Leading singular values vs. wave number for two planar squares in 3D.

half wavelength and the length of each cylinder is 0.4. The separation distance between the two cylinders is one wavelength. The pattern for the number of leading singular values agrees with our high separability result shown in Section 4.2.

6. Conclusion

In this work, the approximate separability of Green's functions of the Helmholtz equations in the high frequency limit, which has direct implications for low rank approximations for the corresponding discretized linear systems, is studied. By characterizing the fast decorrelation between two Green's functions due to fast oscillations in various situations and showing a tight dimension estimate for the approximation of a set of almost orthogonal vectors, we prove explicit and sharp asymptotic estimates for the lower bound and upper bound for the number of terms needed for a separable approximation of the Green's functions of the Helmholtz equation in the high frequency limit. Applications to setups that are commonly used in practice are presented. Numerical tests show agreements with the analysis.

Acknowledgement The authors would like to thank Lawrence C. Evans and Terence Tao for helpful discussions.

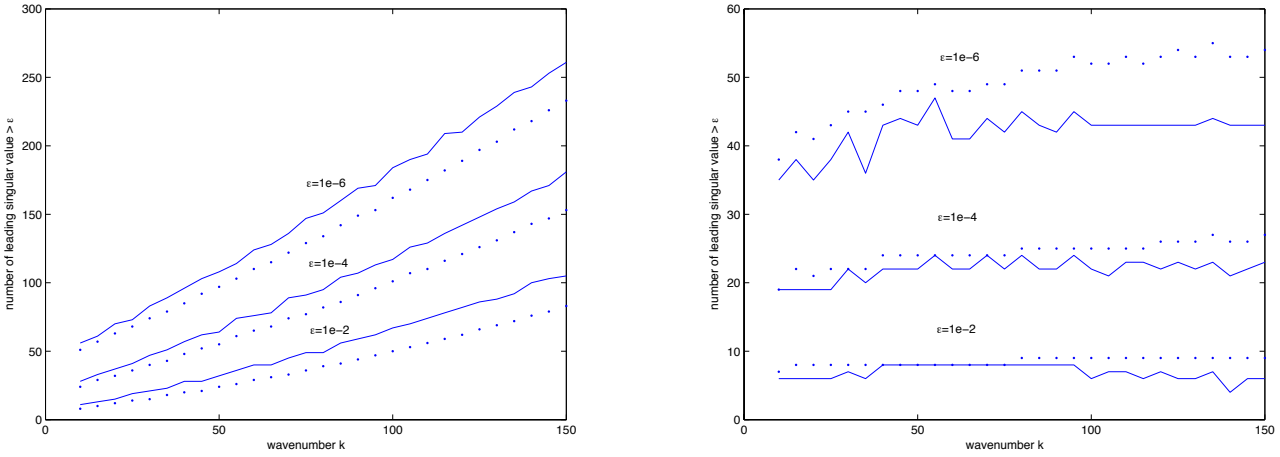

(a) (b)

FIGURE 16. SVD pattern for two spheres and two thin cylinders.

REFERENCES

[1] Noga Alon, *Problems and results in extremal combinatorics, I*, Discrete Math. 273, 31-53, 2003.

[2] M. Bebendorf and W. Hackbusch, *Existence of $\mathcal{H}$-matrix approximants to the inverse FE-matrix of elliptic operator with L^∞-coefficients*, Numer. Math. 95 (2003), no. 1, 1–28.

[3] J.-D. Benamou, F. Castella, T. Katsaounis and B. Perthame, *High frequency limit of the Helmholtz equations*, Rev. Mat. Iberoamericana, 18(1):187?209, 2002.

[4] S. Börm, *Approximation of solution operators of elliptic partial differential equations by $\mathcal{H}$- and $\mathcal{H}^2$-matrices*, Numer. Math. 115 (2010), no. 2, 165-193.

[5] O. M. Bucci and G. Franceschetti, *On the spatial bandwidth of scattered fields*, IEEE Transactions on Antennas and Propagation, Vol 35(12), pp1445-1455, 1987.

[6] O. M. Bucci and G. Franceschetti, *On the degrees of freedom of scattered fields*, IEEE Transactions on Antennas and Propagation, Vol 37(7), pp 918-926, 1989.

[7] E. Candes, L. Demanet, and L. Ying, *A fast butterfly algorithm for the computation of Fourier integral operators*, Multiscale Model. Simul. 7 (2009), no. 4, 1727–1750.

[8] S. Chandrasekaran, P. Dewilde, M. Gu and N. Somasunderam, *On the numerical rank of the off-diagonal blocks of Schur complements of discretized elliptic PDEs*, SIAM J. Matrix Anal. Appl. 31 (2010), no. 5, 2261–2290.

[9] B. Engquist and L. Ying, *Fast directional multilevel algorithms for oscillatory kernels*, SIAM Journal on Scientific Computing 29 (2007).

[10] B. Engquist and L. Ying, *Sweeping preconditioner for the Helmholtz equation: Hierarchical matrix representation*, Communications in Pure and Applied Mathematics 64, 2011.

[11] O. Ernst and M.J. Gander, *Why it is Difficult to Solve Helmholtz Problems with Classical Iterative Methods*, Numerical Analysis of Multiscale Problems, I. Graham, T. Hou, O. Lakkis and R. Scheichl, Editors, pp. 325-363, Springer Verlag, 2012.

[12] L. Greengard and V. Rokhlin, *A fast algorithm for particle simulations*, J. Comput. Phys., vol. 73, pp. 325–348, 1987.

[13] L. Greengard, *The rapid evaluation of potential fields in particle systems*, ACM Distinguished Dissertations, MIT Press, Cambridge, MA, 1988.
[14] M. Grüter and K. -O Wildman, *The Green function for uniformly elliptic equations*, Manuscripta Math. 37 (1982), no. 3, 303–342.
[15] M. Gu and S. Eisenstat *Efficient algorithms for computing a strong rank-revealing QR factorization*, SIAM J. Sci. Comput., 17 (1996), pp. 848–869.
[16] K. Ho and L. Ying, *Hierarchical interpolative factorization for elliptic operators: differential equations*, preprint.
[17] Lars Hörmander, *The Analysis of Linear Partial Differential Operators, I*, Springer-Verlag, 1983.
[18] A. N. Kolmogorov, *Über die beste Annäherung von Funkionen einer Funktionklasse*, Ann. Math,. 37 (1936), 107–111.
[19] S. Luo, J. Qian and R. Burridge, *Fast Huygens sweeping methods for Helmholtz equations in inhomogeneous media in the high frequency regime*, J. Comput. Phys. 270, 378–401, 2014.
[20] W. B. Johnson and J. Lindenstrauss, *Extensions of Lipschitz mappings into a Hilbert space*, Contemp. Math. 26, AMS, Providence, RI, 189-206, 1984.
[21] J. Keller and R. M. Lewis, *Asymptotic methods for partial differential equations: the reduced wave equation and Maxwell?s equations*, Surveys Applied Mathematics,1:1?82, 1995.
[22] W. Littman, G. Stampacchia and H. F. Weinberger, *Regular points for elliptic equations with discontinuous coefficients*, Annali della Scuola Normale Superiore di Pisa - Classe di Scienze, Sér. 3, 17 no. 1-2, p. 43–77, 1963 .
[23] P.-G. Martinsson and V. A. Rokhlin, *A fast direct solver for scattering problems involving elongated structures*, J. Comput. Phys. 221, no. 1, 288–302, 2007.
[24] P.G. Martinsson, V. Rokhlin, and M. Tygert, *A randomized algorithm for the approximation of matrices*, Applied and Computational Harmonic Analysis, 30(1), pp. 47–68, 2011.
[25] P. -G. Martinsson, *A fast direct solver for a class of elliptic partial differential equations*, J. Sci. Comput. 38 (2009), no. 3, 316–330.
[26] E. Michielssen and A. Boag, *A multilevel matrix decomposition algorithm for analyzing scattering from large structures*, IEEE Trans. Antennas and Propagation, 44 (1996), no. 8, pp. 1086–1093.
[27] M. O'Neil, F. Woolfe, and V. Rokhlin, *An algorithm for the rapid evaluation of special function transforms*, Applied and Computational Harmonic Analysis, 28 (2010), no. 2, pp. 203–226.
[28] V. Rokhlin, *Rapid solution of integral equations of scattering theory in two dimensions*, J. Comput. Phys., vol. 86 (1990), pp. 414–439.
[29] V. Rokhlin, *Diagonal forms of translation operators for the Helmholtz equation in three dimensions*, Appl. Comput. Harmon. Anal. 1 (1993), no. 1, 82–93.
[30] J. Roe, *Elliptic operators, topology, and asymptotic methods*, Chapman & Hall/CRC Research Notes in Mathematics Series, 2nd edition, 1999.
[31] P. G. Schmitz and L. Ying, *A fast direct solver for elliptic problems on general meshes in 2D*, J. Comput. Phys. 231 (2012), no. 4, 1314-1338.
[32] András Vasy, *Lecture notes at Stanford University.*
[33] J. Xia, S. Chandrasekaran, M. Gu and X. S. Li, *Superfast multifrontal method for large structured linear systems of equations*, SIAM J. Matrix Anal. Appl. 31(2009), no. 3, 1382–1411.
[34] J. Xia, *Efficient structured multifrontal factorization for general large sparse matrices*, SIAM J. Sci. Comput. 35 (2013), no. 2, A832-A860.

Department of Mathematics, University of Texas and ICES, University of Texas at Austin, 1 University Station C1200, Austin, TX, 78712.
E-mail address: engquist@ices.utexas.edu

Department of Mathematics, University of California, Irvine, CA 92697.
E-mail address: zhao@math.uci.edu